MIT Libraries | DSpace@MIT

MIT Open Access Articles

Assembly and operation of the autopatcher for automated intracellular neural recording in vivo

Massachusetts Institute of Technology

Setting up and using the autopatcher for automated intracellular neural recording *in vivo*

Suhasa B. Kodandaramaiah[1,2,3], **Gregory L. Holst**[4], **Ian R. Wickersham**[1,2,3], **Annabelle C. Singer**[1,2,3], **Giovanni Talei Franzesi**[1], **Michael L. McKinnon**[5], **Craig R. Forest**[4,*], and **Edward S. Boyden**[1,2,3,*]

[1]MIT Media Lab, MIT, Cambridge, MA

[2]McGovern Institute for Brain Research, Cambridge MA

[3]Depts. of Biological Engineering and Brain and Cognitive Sciences, MIT, Cambridge MA

[4]George W. Woodruff School of Mechanical Engineering, Georgia Institute Of Technology, Atlanta, GA

[5]Department of Physiology, School of Medicine, Emory University, Atlanta, GA

Abstract

Whole cell patch clamping *in vivo* is an important neuroscience technique that uniquely provides access to both supra-threshold spiking and sub-threshold synaptic events of single neurons in the brain. This article describes how to set up and use the autopatcher, a robot for automatically obtaining high yield and high quality whole cell patch clamp recordings in vivo. Following this protocol, a functional experimental rig for automated whole cell patch clamping can be set up in one week. High quality surgical preparation of mice takes approximately 1 hour, and each autopatching experiment can be carried out over periods lasting several hours. Autopatching should enable *in vivo* intracellular investigations to be accessible by a significant number of neuroscience labs, and enable labs already doing *in vivo* patch clamp to scale up their efforts by reducing training time for new lab members and increasing experimental durations by handling mentally intensive tasks automatically.

INTRODUCTION

In vivo whole cell patch clamping is an electrophysiological technique that enables high-fidelity measurement of the electrical activity of neurons in the living brain. The high

signal–to-noise ratio and temporal resolution of the recordings enables the measurement of both subthreshold membrane potentials and suprathreshold spiking events[1–4]. Moreover, current can be delivered intracellularly to drive or silence the cell being recorded or to allow characterization of specific receptors or ion channels in the cell. In addition, whole cell patch clamping allows infusion of cell staining dyes to visualize cell morphology, extraction of cell contents for transcriptomic analysis[5] and single cell gene transfection[6]. Since its early application for recording *in vivo*[7], it has been a gold standard technique for the study of intracellular dynamics of single neurons in intact brains[1, 8–16]. It has also been combined with two-photon imaging for targeted patch clamping of identified neurons[17–19]. Multiple groups have demonstrated the use of *in vivo* patch clamping for recording in awake freely moving animals[20–23]. However, manual whole cell patch clamping is a laborious technique and is considered something of an art form, especially when performed *in vivo*. Manual whole-cell patch clamping has proven difficult to automate, and therefore has had low yield and throughput. We recently discovered a different method for *in vivo* patch clamping that was simple to automate[24]. In our method, we detect neurons by lowering a pipette in small (e.g., 2 µm) steps, and perform a time series analysis of the resistance of the patch pipette as it is lowered into the brain, looking for a small, but monotonic, increase in pipette resistance that takes place over several consecutive steps. This differs from previous methods of neuron detection *in vivo*, which utilize human-detectable changes, e.g. large jumps in resistance, or appearance of fluctuations in the pipette signals due to heartbeat[7, 25], and may contribute to the high performance of our method when performed in an automated fashion. This protocol article provides further practical details on setting up the autopatcher, as well as the procedure for using the autopatcher to obtain whole cell recordings in the live mammalian brain.

Automating *in vivo* whole cell patch clamp

The autopatching algorithm breaks down the process of whole cell patch clamping into six stages (Fig. 1a). The autopatcher conducts an initial assessment of the suitability of an installed pipette for patch clamping ('Pipette assessment outside the brain'). Then the autopatcher rapidly lowers the patch pipette to the desired recording area ('Regional pipette localization') with the pipette interior at high positive pressure to prevent tip clogging. This is followed by the 'Neuron hunting' stage, in which the pipette is advanced in small increments at a lower pressure while constantly monitoring the pipette resistance until a neuron is detected, as indicated by a specific temporal sequence of pipette resistance changes. Once a neuron has been detected, the 'Gigaseal formation' stage is executed, during which negative pressure and hyperpolarizing current are applied to the pipette to attempt to form a seal with the targeted cell's membrane. Finally, in the 'Break-in' phase, brief pulses of negative pressure and/or voltage are applied to rupture the patch of membrane at the pipette tip to obtain the whole-cell configuration.

The autopatcher executes this algorithm by assuming position, pneumatic and electric control of the patch pipette (Fig. 1b). Position control of the patch pipette is achieved by using a programmable linear motor. A "digitizer" board equipped with analog inputs, as well as analog and digital outputs, in a custom-built control box interfaces with the patch amplifier to acquire and log pipette impedance measurements throughout the autopatching

process, and controls the application of hyperpolarizing current during gigasealing. The control box also includes an electronic pressure regulation system that can apply positive and negative pressures to the pipette at various stages of autopatching. Included with this protocol is the autopatcher software (Supplementary Data 1), which executes the algorithm. The success rates seen when using our robot are similar to those obtained by trained humans. Whole cell patch clamping in anesthetized mice is successful in ~32% of the trials on average, with greater than 60% of the trials yielding good recordings in a freshly opened craniotomy[24]. Thus, for investigators starting to do *in vivo* whole cell patch, our robot may facilitate entry into the field. Robots do not suffer from fatigue and may thus be of use even for trained *in vivo* patch clamp electrophysiologists seeking to increase robustness and yield for lengthy experiments.

Overview of autopatcher hardware and software

The general layout of the autopatcher equipment is shown in Figure 2. The core components of the autopatcher setup include the patch amplifier, a signal digitizer board equipped with analog inputs, as well as analog and digital outputs, for data acquisition and control, a custom autopatcher control box, and a pipette actuator for manipulating the patch pipette. The pipette actuator along with the amplifier headstage and custom head fixation base for immobilizing the mouse are installed on an optics table (or other sturdy table that is isolated from mechanical vibrations and electrical noise) (Fig. 2a and c). The pipette actuator allows programmatic control of the patch pipette movement in the axial direction during autopatching. In the current implementation (Fig. 2c) this is achieved by mounting a programmable linear motor (PT1-Z8 motor with TDC001 controller, Thorlabs) onto a manually controlled 3-axis linear stage (MPC285, Sutter Instruments).

The autopatcher equipment described here has been improved over that described in 2012. The key difference between the current version and the original 2012 version[24] is the use of an electronic control box instead of a manual syringe for pressure control. This control box also interfaces with the patch amplifier and the traditional external data acquisition device/ digitizer (required for patch clamp amplifier operation; Fig. 2b and d). The control box takes in a steady high pressure air supply (~2580 mBar) and downregulates it to two discrete positive pressures (high positive pressure of 1000 mBar and low positive pressure of 100 mBar). Two discrete negative pressures states (high negative pressure of −350 mBar and low negative pressure of −25 mBar) are also generated from the same steady high-pressure air input using Venturi tube vacuum generators. Finer control of these pressures is then achieved by using electronic pressure regulators which can modulate the pressures (0 to 800 mBar high positive pressure, 0 to 25 mBar low positive pressure, −25 to 0 mBar low negative pressure and −350 to 0 mBar high negative pressure) using potentiometers mounted on the control box's front panel. These pressures are inputs to a bank of 3-way valves. Digital TTL signals from the digitizer board switch the individual valves to change which pressure is applied to the pipette during autopatching.

The digitizer board inside the control box connects to the computer via a USB interface. It has one analog output channel dedicated to sending command signals to the patch amplifier during autopatching. An internal relay is used to switch the command signals sent to the

amplifier from the internal digitizer or the traditional external digitizer to enable experimental flexibility (Fig. 2d). One analog input channel is used to record the current or voltage output signal from the patch amplifier. These measurements are used to compute the pipette resistances while the autopatching algorithm is being executed. The amplifier output is split within the box and routed to the traditional external digitizer as well as the internal one. These improvements in the pressure delivery system necessitated changes to the 2012 software interface. While the algorithm used for autopatcher is the same as that described in our 2012 paper[24], the software has been modified to interface with the new hardware configuration. The current software program also includes scripts for controlling the amplifier software within the autopatcher program using dynamic link libraries (.dll) (Supplementary Data 1). Some of the materials included in this protocol (specifically, the software) were previously posted at the website http://autopatcher.org; going forward, we will post periodic updates to the software and hardware on this site.

The rationale for including an extra linear motor, in addition to the software-controllable Sutter manipulator, and an internal digitizer, in addition to the traditional external digitizer, is to enable modularity. That is, we wanted to design a system that could be added easily to an existing patch rig, to make it automated. Of course, motors that can be directly controlled by computer (for example the Sutter manipulator) or external digitizers that allow external software access, may be directly modified by end users, and in such cases one could ignore the additional motor and digitizer. But here we focus on a modular toolbox that, in principle, could be added to any existing patch system to make it automated.

Experimental Design

The protocol for setting up an autopatcher and performing automated whole cell patch clamping *in vivo* is divided into six stages. **Stage I – Hardware Setup** has detailed instructions for constructing, calibrating and testing autopatcher-specific hardware (**Steps 1–6**). This is followed by **Stage II – Software Setup** which guides the user on configuring the autopatcher software to control the autopatcher hardware components (**Steps 7–11**). **Steps 1–11** are one-time installation instructions that setup a fully functional autopatcher rig. The subsequent steps involve instructions for each individual experiment. The setup of the autopatcher rig involves integrating off-the-shelf and custom components into an otherwise standard *in vivo* electrophysiology rig. Some of these integration steps require custom parts. The mechanical drawings and computer aided design (CAD) files of all these custom parts are provided in the supplementary material (Supplementary Data 2, 3 and 4) and can be used to fabricate them in-house or can be sent to a commercial fabrication service (such as http://www.e-machine.com) to be made.

The step-by-step protocol for high quality surgical preparation of mice for autopatching is described in **Stage III – Surgical preparation: Headplate attachment and craniotomy** (**Steps 12–20**). The beginning of each autopatching experiment requires initialization and configuration of the autopatcher software (**Stage IV – Initializing software programs for autopatching**, **Steps 21–24**). The experimenter can then follow the steps in **Stage V – Setting up the autopatcher for patch clamping trial** to setup the autopatcher for each autopatching trial (**Steps 25–31**).

The procedure followed by the autopatcher to automatically obtain whole cell patch clamp recordings is described in Box 2 – **Autopatching**. The experimenter can follow the progress of autopatching by observing the autopatcher software graphical user interface (GUI). The GUI incorporates interactive features to guide users through these stages, with pop-up dialog boxes appearing when an end point has been reached or when other user input is required. In a successful trial, no input is needed from the experimenter until a whole cell recording or cell-attached recording is obtained (**Step 36**). However, in some trials, the autopatcher may reach an end point prior to obtaining a whole cell recording that requires user input (e.g., if the pipette is found to be unsuitable for autopatching). In such cases, the pop-up dialog boxes will guide the experimenter on how to restart the trial (**Step 32–34**). At any point, if the experimenter wishes to start a new trial from **Step 24**, the **'START OVER'** button can be pressed to stop the current trial and bring the pipette back to the brain surface for retrieval. The entire autopatching process is shown in Supplementary Video 1. The experimenter can then follow the instructions in **Stage VII – Whole cell recording and recovery after biocytin filling** for obtaining voltage and current clamp recordings after a successful autopatching attempt (**Steps 37–39**).

Before any *in vivo* experiments are attempted, it is recommended that the experimenter first perform a practice run of the autopatcher with the pipette tip immersed in a saline bath as a proxy for an *in vivo* experiment. This will allow the experimenter to get familiar with the autopatcher hardware and software systems, and troubleshoot any equipment issues before an *in vivo* experiment is attempted. A modified, alternate protocol for doing a practice run in a saline bath (in lieu of **Steps 21–39** detailed below) is described in the Supplementary Method.

This protocol is written with the assumption that the experimenter has some familiarity with the basic principles of patch clamp physiology and rodent surgery. Prior experience setting up an experimental electrophysiology rig and denoising it (e.g., for obtaining high-quality patch clamp recordings) is helpful. The autopatcher has been tested extensively in the cortex and hippocampus in anesthetized mice[24], and although the protocol is written with the mouse in mind it can also be applied, in principle, to a variety of species, brain regions, and experimental contexts[26]. It is highly recommended that autopatcher users acquaint themselves with the existing *in vivo* patch clamping literature and protocols (e.g.,[19, 24, 25, 27, 28]) to obtain a full understanding of the best practices that have enabled other research groups to get consistent *in vivo* electrophysiology results. As with any patch clamp experiment, obtaining high yield and high recording quality with the autopatcher is contingent on pristine experimental preparation – environmental cleanliness, solution purity and accuracy, and surgery quality (e.g., solid headplate attachment to skull, excellent craniotomy quality). It is also critical to ensure proper cleanliness of the working area since any dirt, dust, or contamination can clog what should be extremely clean pipettes, or otherwise impair recording quality. Successful patching also relies on high quality patch pipettes, freshly pulled according to an optimized and robust protocol.

MATERIALS

Reagents

Mice and surgery—Anesthesia cocktail. For example a mix of 100 mg/kg of ketamine and 10 mg/kg of xylazine, or 1–2% isoflurane in oxygen, or other approved anesthetic obtained from the institutional veterinarian.

1.1.2 Dental cement (e.g., Stoelting, # 51458)

1.1.3 Sterile saline (e.g., VWR, # 101320-574)

1.1.4 Lidocaine (e.g., VWR, # 95033-980)

1.1.5 Puralube ophthalmic ointment (e.g., Dechra, # 17033-211-38)

1.1.6 Betadine (e.g., McKesson, # 521234)

1.1.7 70% ethanol (e.g., VWR, # 71001-654)

1.1.8 Sterilized cotton swab (e.g., Coviden/Kendall, # 61541400)

1.1.8 Animals: C57BL/6 mice, 8–12 week old mice (e.g., Taconic, # B6-M), male or female, although other strains of mice can also be used.

> **CAUTION:** All animal use must comply with institutional and national regulations.

1.2 Electrophysiology Supplies

1.2.1 Potassium gluconate (e.g., Sigma Aldrich, # P1847)

1.2.2 $CaCl_2$ (e.g., Sigma Aldrich, # C1016)

1.2.3 $MgCl_2$ (e.g., Sigma Aldrich, # M8266)

1.2.4 EGTA (e.g., Sigma Aldrich, # E3889)

1.2.5 HEPES (e.g., Sigma Aldrich, # H3375)

1.2.6 Mg-ATP (e.g., Sigma Aldrich, # A9187)

1.2.7 Na-GTP (e.g., Sigma Aldrich, # G8877)

1.2.8 NaCl (e.g., Sigma Aldrich, # S3014)

1.2.9 Sucrose (e.g., Sigma Aldrich, # S0389)

1.2.10 Biocytin (e.g., Sigma Aldrich, # B4261)

1.2.11 HCl (e.g., Sigma Aldrich, # H1758)

1.2.12 KCl (e.g., Sigma Aldrich, # P9541)

1.2.13 NaH_2PO_4 (e.g., Sigma Aldrich, # S8282)

1.2.14 $MgSO_4$ (e.g., Sigma Aldrich, # M2643)

1.2.15 $NaHCO_3$ (e.g., Sigma Aldrich, # S5761)

1.2.16 Glucose (e.g., Sigma Aldrich, # 49163)

1.2.17 Low gelling temperature agarose (e.g., Sigma Aldrich, # A9414)

1.2.18 Glass capillaries (e.g., Warner, # 64-0790)

1.2.19 Bleach (e.g., VWR, # 66025-688)

1.2.20 De-ionized water (e.g., Life Technologies, # AM9937)

1.2.21 KOH (e.g. Sigma Aldrich, #P5958)

1.2.22 Bottle top vacuum filter (e.g., Nalgene, # 292-4520)

1.2.23 1ml syringe (e.g., Becton, Dickinson and Company, # 301025)

1.2.24 0.20 μm syringe filter (e.g., VWR, # 97048-592)

2. Equipment

2.1. Equipment and tools for surgery

2.1.1 Stereotax (e.g., Kopf, Model 900)

2.1.2 Cold light source for surgery station (e.g., Leica, L2)

2.1.3 Self-tapping skull screws (e.g., Morris Precision Screws and Parts, # F000CE094)

2.1.4 Custom headplate (Needs to be fabricated in house or by a custom supplier; the template is in Supplementary Data 2 – **'Headfixation.zip'**, and is entitled **'Head Plate CAD.sldprt'**)

2.1.5 No. 10 surgical blade, (e.g., Swann Morton, # 0501)

2.1.6 Micro curette (e.g., Fine Science tools, # 10080-05)

2.1.7 Hair trimmer (e.g., Wahl, # 8786)

2.1.8 Dental drill (e.g., Pearson Dental, # G24-00-05)

2.1.9 500 μm drill bit (e.g., Pearson Dental, # P86-02-38)

2.1.10 27 gauge needles (e.g., Becton Dickinson, # 305109)

2.1.11 31 gauge needles (e.g., Becton Dickinson # 328438)

2.1.12 Stereomicroscope for surgery station (e.g., Leica, # M60)

2.1.13 Rodent temperature control system (e.g., Fine Science Tools, TR200)

2.1.14 Ag-AgCl ground electrode pellet (e.g., Warner Instruments, # 64-1305)

2.1.15 Sterile absorbent paper points (e.g., World Precision Instruments, # 504180)

2.1.16 Inline solution filter (e.g., VWR, # 66064-826)

2.1.17 Scalpel handle #3 (e.g., Fine Science Tools, # 10003-12)

2.1.18 Scissors (e.g., Fine Science Tools, # 14060-09)

2.2. Equipment and tools for autopatching

2.2.1 Patch amplifier (e.g., Molecular Devices Inc., Multiclamp 700B)

2.2.2 Signal digitizer (e.g., Molecular Devices Inc., Digidata 1440B)

2.2.3 Data acquisition software (e.g., Molecular Devices Inc., Clampex)

2.2.4 Amplifier control software (e.g., Molecular Devices Inc., Multiclamp Commander)

2.2.5 Desktop computer (Microsoft Windows operating system with at least 4GB RAM, dual core processor, 1024×768 resolution display)

2.2.6 Autopatcher control software (Supplementary Data 1-**'Autopatcher Software.zip' or** www.autopatcher.org)

2.2.7 LabVIEW software (National Instruments LabVIEW 2011 or later version)

2.2.8 Vibration isolation table with Faraday cage (e.g., TMC, # 63-531)

2.2.9 3-axis manipulator (e.g., Sutter Instruments, MP285)

2.2.10 Linear motor with controller (Thorlabs, PT1-Z8, TDC001, TPS001)

2.2.11 Assorted mechanical components (Thorlabs, DP14A, MB4, C1505)

2.2.12 Custom mechanical parts (See Supplementary Data 3 – **'Autopatcher Pipette Actuator.zip'** that contains files entitled **"Adaptor plate 1.SLDPRT"** and "**Adaptor plate 2.SLDPRT"**)

2.2.13 Custom head fixation holder (**See** Supplementary Data 1 **'Head fixation.zip'** and use **'Head fixation base CAD.sldprt'** for 3-D printing the part or procure from commercial 3D printing service such as www.i-materialize.com).

2.2.14 Autopatcher pressure control box (e.g., Neuromatic Devices or see the assembly manual in Supplementary Data 4 – **'Autopatcher control box.zip'**)

2.2.15 Low noise rodent temperature monitor and controller (e.g., FHC 40-90-8D)

2.2.16 Pipette holder (e.g., Molecular Devices, HL-U-1)

2.2.17 Pipette puller (e.g., Sutter Instruments, P97)

2.2.18 Microfil (e.g., World Precision Instruments, # MF28G67-5)

2.2.19 Cold light source for autopatcher setup (e.g., Leica, L2)

2.2.20 Stereomicroscope for autopatcher setup (e.g., Leica # M60)

2.2.21 Ag-AgCl ground electrodes (e.g., Warner Instruments, # 64-1304)

2.2.22 Socket head cap screw assortment (e.g., Mcmaster Carr, # 92085A224)

2.2.23 1.59 mm (1/16th inch) thick Delrin sheet (e.g., Mcmaster Carr, # 8573K31)

2.2.24 Table clamps (e.g., Thorlabs, CL5)

2.2.25 100–150 μm diameter silver wire (e.g., Warner Instruments, # 64-1318)

2.2.26 Ag-AgCl pellets (e.g., Warner Instruments, # 64-1309)

2.2.27 1 mm gold coated pins (e.g., Warner Instruments, # 64-1325)

2.2.28 Manometer (e.g., Dwyer, #475-5-FM)

2.2.29 Assorted Luer fittings (e.g., Cole-Parmer, # EW-45511-00)

2.2.30 Helping hands (e.g., Amazon, # SE MZ101B)

2.2.31 Non deformable 3.175 mm (1/8th inch) outer diameter tubing (e.g. McMaster Carr, # 5779K677)

2.2.32 Non deformable 6.35 mm (1/4th inch) outer diameter tubing (e.g., McMaster Carr, # 5648K251)

2.2.33 Heat shrink tubing 2.4 mm (3/32nd inch) diameter (e.g. Mouser, 5174-13321)

REAGENT SETUP

Intracellular Pipette Solution

We typically use the following recipe, making around 50 mL at a time. Prepare solution containing (in mM) 135 potassium gluconate, 0.1 $CaCl_2$, 0.6 $MgCl_2$, 1 EGTA, 10 HEPES, 4 MgATP, 0.4 Na GTP, 8 NaCl, as well as 0.5% w/v of biocytin. Adjust the pH to 7.2 by dropwise addition of 5M KOH (for a larger solution volume, e.g. 500 mL, adding increments of 10–30 μl of 5M KOH at a time may work well, lowering the concentration of the base stock solution (e.g., to 1M KOH) as the pH measurements approach the desired value). Then increase the osmolarity of the solution to 290–295 mOsm by iteratively adding small increments (e.g., 25–50 mg at a time) of potassium gluconate. Filter the solution using a bottle top vacuum filter (0.2 μm pore size) and aliquot into 1–1.5 ml volume tubes and store at −80°C. This solution can be stored at −80°C for a few months. Use freshly thawed solution kept on an ice bath during experiments. Refreezing and reuse of unused solution is discouraged.

Artificial Cerebrospinal Fluid

Prepare artificial cerebrospinal fluid (ACSF) consisting of (in mM): 135 NaCl, 2.5 KCl, 10 HEPES, 2 $CaCl_2$ and 1 $MgCl_2$. Adjust the pH to 7.3 by dropwise addition of NaOH and adjust osmolarity to ~300 mOsm by iteratively adding small quantities of NaCl (up to 150 mM final concentration). Filter the solution using a bottle top vacuum filter (0.2 μm pore size) and store the solution at 4°C for up to a few months; warm to 37°C in a clean water bath before use in the experiment.

Patch pipettes

Pull pipettes with resistance between 5–7 MΩ using the pipette puller (Fig. 3). A good starting point is to use patch pipette geometries that have already been proven to work in brain slices, or otherwise empirically optimized. Refer to Box 1 for a description of the ideal pipette geometry that gives optimum autopatching in our laboratory.

PROCEDURE

Hardware Setup

1   **Autopatcher pipette actuator:** Follow the instructions in the assembly manual in Supplementary Data 3 and install the pipette actuator on an optics table (Fig. 2c). Isolate the optics table from mechanical vibrations and electrical noise (Fig. 2a).

2   **Autopatcher control box:** Follow the instructions in the assembly manual in Supplementary Data 4 to assemble and test the autopatcher control box. Assembling the autopatcher control box requires proficiency in electronic and mechanical fabrication. Alternately, a fully assembled control box can be procured from a commercial vendor (e.g., Neuromatic Devices). Connect the pneumatic pressure output on the front panel of the control box to the pipette holder's pressure input using 3.175 mm (1/8th inch) outer diameter non-deformable tubing and barbed Luer fittings as necessary. Connect the USB cable from the box to the computer and connect the BNC connections on the front panel to the patch amplifier and traditional external digitizer (Fig. 2b and d).

3   **Headplate fabrication:** See Supplementary Data 2 and use the **'Head Plate CAD.sldprt'** file to cut the headplates from 1.59 mm (1/16th inch) thick Delrin sheet using a laser cutter. Alternately, the fabricated headplates can be commissioned from commercial fabrication service providers. Use a high speed rotary tool (e.g., Dremel) with a cylindrical sanding attachment to sand the bottom of the headplate to define a curved contour along the headplate window that mates with the curved surface of the mouse skull (Fig. 4a).

4   **Head fixation base fabrication:** See Supplementary Data 2 and use **'Head fixation base CAD.sldprt'** to 3D print the head fixation base in acrylonitrile butadiene styrene (ABS) plastic using a 3D printer. Alternately, the custom head fixation base can be commissioned from a commercial 3D printing vendor. Install the head fixation base on the optics table underneath the autopatcher pipette actuator and clamp securely in position using bolts or table clamps (Fig. 2c).

> **CRITICAL STEP**: Secure clamping is very important. The custom headplates are surgically attached to the skull with dental cement and are then fastened to this base at the beginning of the experiment. If the base is not secured, then motion from the mouse or other disturbances could cause the skull to move relative to the pipette. This will significantly reduce yield and recording stability.

5   **Ground electrode:** Take an insulated wire, 300–450 mm long, and solder a Ag-AgCl pellet on one end and a 1 mm gold coated pin on the other end. Cover soldered sections with insulating heat shrink tubing and shrink it using a heat gun. Plug the gold-coated pin into the back of the amplifier headstage. The Ag-AgCl pellet is kept on top of the skull, submerged in the ACSF bath during the patch experiment using a "helping hand" device (**Step 25** in the protocol).

6   **Ag-AgCl pipette electrode wire:** Take a 50 mm long silver wire and immerse 25 mm of its length in bleach for 5–10 minutes to make the Ag-AgCl pipette electrode. Clean it thoroughly with filtered deionized water and connect the non-bleached end to the gold pin at the top of the pipette holder. Install the pipette holder with the Ag-AgCl wire in the amplifier headstage.

Software Setup

7   **Patch amplifier and data acquisition software:** Install the data acquisition software (e.g., Clampex, Molecular Devices), and the patch amplifier control software (Multiclamp Commander, Molecular Devices). Connect the amplifier and external digitizer directly to the USB ports on the computer. Do not connect them through a USB hub or splitter. In the amplifier control software, configure the feedback resistor to 500 MΩ for both voltage and current clamp. Set the "External Command Sensitivity" to 20 mV/V and 400 pA/V for voltage and current clamp respectively.

8   **Autopatcher software installation:** First install the LabVIEW programming environment (National Instruments, LabVIEW 2011 version or later), as the freely available autopatcher code is written in this environment. Also install the latest data acquisition drivers (DAQmx, National Instruments). Next, download and open Supplementary Data 1. This contains all the code necessary to run the autopatcher in LabVIEW. Updates for this software can be found at www.autopatcher.org. Open the **'Autopatcher 2000.llb'** file within Supplementary Data 1 with LabVIEW to show a list of all the ".vi" files used in the code. Open the **'Autopatcher 2000.vi'** file within **'Autopatcher 2000.llb'** and you should see the graphical user interface (GUI) used to control the autopatcher (Fig. 5).

9   **Programmable motor software:** Install the drivers and software provided by the manufacturer for controlling the programmable linear motor. If using the TDC001 motor controller from Thorlabs, this is the APT controller software.

10   **Configuring Autopatcher Software:** Follow the instructions in the configuration manual '**Autopatcher software configuration manual.pdf**' in Supplementary Data 1 to configure the autopatcher software to recognize and control the programmable motor, internal digitizer, and amplifier software.

11   **Restart the computer:** Restart the computer after completing all the software installations to allow the operating system to register all the changes.

         PAUSEPOINT: This completes the setup of the autopatcher hardware and software. The following steps describe the protocol for performing the *in vivo* experiment. Prior to this, it is recommended that the experimenter follow the steps described in Supplementary Note 1 to test the autopatcher function using a pipette navigating in a saline bath as a proxy for the intact brain. Beyond this initial setup, it is also important to clean the pipette holder, silver wire, ground wire, pipette storage box, and pipette puller bars with ethanol and filtered

deionized water at least monthly to reduce clogging from precipitates and dust accumulation.

Surgical preparation: Headplate attachment and craniotomy

12   **Anesthetize the mouse:** Anesthetize a mouse using an approved anesthesia protocol. We typically use a cocktail of 100 mg/kg of ketamine and 10 mg/kg of xylazine, or 1–2% isoflurane in oxygen. Maintain the animal's anesthetic plane throughout surgery and recording by regularly testing the depth of anesthesia and adjusting anesthetic dosing according to the approved animal protocol.

    CAUTION: All procedures involving animals must be performed in strict compliance with institutional and federal regulations concerning laboratory animals. The procedure we describe here was approved by the Division of Comparative Medicine (DCM) at the Massachusetts Institute of Technology.

13   **Prepare the mouse for surgery:** Apply ophthalmic ointment to the eyes, and use hair trimmers and scissors to trim hair on top of the head (Fig. 4b) to prepare the scalp for incision. Scrub the head with a sterile cotton swab soaked in betadine, followed by scrubbing with 70% ethanol to clean the scalp (repeat ~3 times as required). Ensure all hair clippings are removed from the surgical area during this procedure.

14   **Fix the mouse in stereotaxic apparatus:** Fix the mouse in the stereotaxic apparatus using the ear and mouth bars. Adjust the ear bars and nose cone of the stereotax such that bregma and lambda reference points are at the same height and the midline is parallel to the anteriopoterior axis of the stereotax frame. Ensure the mouse is placed on a heating pad with a temperature probe to regulate body temperature during the surgical procedure.

15   **Incise the scalp and expose the skull:** Using a #10 surgical blade, make a clean longitudinal incision (anterior to posterior) (Fig. 4c). Use small retractors to pull apart the skin over the skull. Use a micro curette to remove fascia. Identify the location for the craniotomy using the stereotaxic coordinates (Fig. 4d). Using a burr drill bit, gently make a burr hole at the spot to mark the location of the craniotomy. Do not drill all the way through the skull.

16   **Implant the skull screws:** Using a dental drill, drill three anchor holes (~500 μm diameter) into the skull. Screw in the self-tapping skull screws into the drilled holes (indicated by the three small red dots in Fig. 4e). The location of the skull screws should be made so that the desired recording craniotomy location is roughly centered inside the headplate window. Place two posterior skull screws and one anterior skull screw with approximately 7 mm between the anterior and posterior positions so that when the headplate is fixed the skull screws are just inside the 'window' of the headplate.

17   **Attach the headplate:** Clamp the headplate to the stereotaxic arm so that it is horizontal in the stereotax frame and then lower the stereotaxic arm until the headplate sits on the exposed skull. Apply freshly mixed dental acrylic cement

around the skull screws and around the periphery of the headplate (Fig. 4f). Do not apply the acrylic cement over the craniotomy location. This should cure in 10–15 minutes. Picture of the skull surface before and after the headplate attachment is shown in Figure. 4g.

18   **Open the craniotomy for recording:** Gently mill down the surface of the skull, in a circular area approximately 1 mm in diameter, until the bone tissue is thin enough to appear flaky and translucent (Fig. 4h and Fig. 4i). Then use a 31-gauge needle to pick away at the desired point on the thinned skull very gently, opening up a single small hole approximately 500 μm in diameter, inducing minimal brain exposure (Fig. 4j and Fig 4k). Keep the brain surface wet with ACSF while attempting to open the craniotomy. Good technique for opening craniotomies has been previously described by Lee et al[20]. Ensure the craniotomy has been cleared of all bone debris, before proceeding to the next step.

> **CRITICAL STEP:** The size and quality of the craniotomy has a significant influence on the yield and success rate of autopatching. This has been well documented by other groups performing manual *in vivo* whole cell patch clamping[20].
>
> Make sure that the surface of the brain is not damaged when attempting to dislodge and lift off the bone.

19   **Perform a durotomy:** Use a 31 gauge needle to cut a 100–500 μm slit in the dura while keeping the tip of the needle pointing tangentially to the surface of the brain to prevent damaging the brain. Using the needle or fine forceps, slowly fold the dura to either side of the incision to create an opening. Bleeding can be controlled with sterile absorbent pads or by perfusing the craniotomy with ACSF. This step should be done with caution if there are major blood vessels present.

20   **Head fix the mouse in the autopatcher:** Once surgical preparation is complete, secure the mouse to the custom head fixing base in the autopatcher (Fig. 2c) by fastening the headplate to the mouse head fixation base using #4–40 socket head screws. Keep the mouse on a heating pad to ensure that the body temperature is regulated throughout the autopatching experiment.

Initializing software programs for autopatching

21   **Start the amplifier control software:** Open the amplifier software (e.g., Multiclamp Commander). The amplifier software should automatically recognize the amplifier connected to the computer. Set the correct channel of the amplifier to voltage clamp mode.

22   **Start the data-acquisition software:** Open and run the data acquisition software (e.g., Clampex, Molecular Devices) to monitor and record the currents measured during the experiment.

23   **Start the autopatcher software:** Open the **'Autopatcher 2000.vi'** in LabVIEW and click the **'RUN'** button (see Supplementary Data 1). The autopatcher will initialize the control box and a new LabVIEW program window with the motorized manipulator controls will appear in 30–40s.

24   **Start a new trial in the autopatcher software:** Set the recording depth at which you want the autopatcher to start searching for neurons in the **'Pipette depth to begin neuron hunting (micrometers)'** numerical entry box and set the depth at which you want the autopatcher to stop searching for neurons in the **'Pipette depth to stop neuron hunting (micrometers)'** numerical entry box (Fig. 5). Click the **'BEGIN NEW TRIAL'** button. A pop-up dialog box will appear instructing the experimenter to install a new pipette for autopatching. Throughout the operation of the software, Panel 4 of the GUI (see Fig. 4) will change periodically to report the most current information or collect input from the user that is appropriate for the current stage (Supplementary Video 1).

D. Setting up autopatcher for autopatching trial

25   **Install ground electrode:** Place the ground wire's Ag/AgCl pellet on top of the skull close to the craniotomy.

>   **CRITICAL STEP**. During operation, ensure that the ground wire Ag/AgCl pellet is submerged in the ACSF solution above the skull surface and is not subject to any mechanical motion.

26   **Inspect the craniotomy:** Perfuse the craniotomy with sterile ACSF if needed to clean the surface (e.g., of any residual blood).

27   **Install a pipette in the autopatcher:** Fill a patch pipette with internal pipette solution using a syringe filter and Microfil and install in the pipette holder.

>   **CRITICAL STEP:** Always use a fresh, unused pipette for every trial. Do not attempt to re-use patch pipettes from a previous trial.

>   To achieve a closed circuit connection, ensure that there is sufficient solution in the pipette to submerge a portion of the Ag-AgCl wire when the pipette is installed in the pipette holder.

>   Ensure the internal pipette solution is kept on an ice bath for the duration of the experiment and is filtered (0.2 μm pore size) before backfilling the pipette to prevent internal clogging of pipettes. It is recommended to use the pipettes within a few hours of pulling.

28   **Set pressure states in the autopatcher control box:** Adjust the autopatcher control box pressures by adjusting the knobs on the control box's front panel. Set the high positive pressure to 800 mBar, low positive pressure to 25 mBar, low negative pressure to −15 mBar, and high negative pressure to −300 mBar.

29   **Position the pipette for autopatching:** Carefully position the tip of the patch pipette 20–30 μm above the brain surface using the manual 3-axis manipulator. The size of the craniotomy, and the pipette, and other known quantities, can

serve as a "scale bar" for this process. During this procedure, maintain a thin (5–30 μm) film of fluid over the surface of the brain to prevent the tissue from drying out. Use the stereomicroscope to visualize the pipette tip and craniotomy in this step. Measurements of depth traversed by the autopatcher in subsequent steps are referenced from this starting position. After the tip is positioned, add ACSF until both the tip of the patch pipette and the ground pellet are submerged. This will complete the circuit.

30   **Monitor currents and de-noise the autopatcher:** Observe the currents being measured by the amplifier in the data acquisition software. Eliminate any sources of 60 Hz (or 50 Hz depending on geographical region) electrical noise. This can be done by grounding the Faraday cage and the vibration isolation table to the signal ground of the patch amplifier, identifying sources of noise such as microscope lamps and power supplies and either shielding them, powering them down, or relocating them outside the Faraday cage. Shielding the headstage with metal foil and the space surrounding the silver wire may also help. All metal foil shielding should be connected to the optic table ground. The peak-to-peak noise level in the current measurement should be less than 40pA. This completes the manual setup stage of an autopatching trial.

31   **Begin an autopatching trial:** Click **'OK'** in the pop-up dialog box in the autopatcher GUI (referred to in **Step 24**). The autopatcher will now perform automated whole cell patching until the point when the experimenter choses to either record in whole cell or cell attached mode. These automatically performed steps are described in Box 2 (see also Figures 5–7). Some of these automatic steps may result in outcomes that require user intervention. **Steps 32 and 33** describe what to do if such conditions are encountered.

Step 32   **User intervention if pipette is found to be unsuitable for autopatching** (BOX 2, **Autopatching Step 1**): Click **'OK'** to stop the autopatcher program. Restart a new trial from **Step 24**. This step is not required if the autopatcher proceeds to **Autopatching Step 2**.

Step 33   **User intervention if pipette gets clogged, fouled or broken during descent to recording depth** (BOX 2, **Autopatching Step 2**): Click **'OK'** to stop the autopatcher program. Restart a new trial from **Step 24**. This step is not required if the autopatcher proceeds to **Autopatching Step 3**.

Step 34   **User inputs during gigasealing** (BOX 2, **Autopatching Step 5**): If a cell-attached recording is desired, click **'NEXT'** to proceed to recording and proceed to **Step 37**. If whole-cell recording is desired, proceed to **Step 35**.

Step 35   **Confirming gigaseal formation:** Check that a successful gigaseal has been obtained (BOX 2, **Autopatching Step 5.ii**). If it has, proceed to step 36. If it has not and you wish to start a new trial, click **'START OVER'** to stop the current trial and start a new trial from **Step 24**.

Step 36   **Break-in:** Press the **'ATTEMPT BREAK IN'** button to break into the gigasealed neuron. The autopatcher applies a high negative pressure pulse,

followed by an assessment of the membrane resistance to detect a successful break-in. The holding current required to hold the cell at −65 mV in voltage clamp after each break-in attempt is updated in the '**Holding Current (pA)**' report boxes. The current trace corresponding to the injection of a 10 mV voltage square wave after a break-in attempt is plotted in the '**WHOLE CELL CURRENTS MONITOR**' graph (Fig. 7c). If whole cell patch clamping is not obtained, proceed to option A. If a whole cell patch clamp recording is obtained proceed to Option B. For a typical mouse cortical pyramidal neuron, successful break-in indicated by a membrane resistance <200 MΩ and current injection required to voltage clamp the patched cell at −65mV of <200 pA which occurs in greater than 80% of successful gigaseals[24]. A representative screenshot of the current trace plotted in the '**WHOLE CELL CURRENTS MONITOR**' graph after a successful break-in attempt is shown in Fig. 7c.

Option A) Whole cell patch clamp recording is not obtained.

i.   We recommend you attempt the break-in process 1–5 times, with increasing negative pressure pulse duration (250, 500, 750 and 1000 ms durations) Alternatively, use the '**ZAP!**' button to attempt break-in, which applies a 250 mV amplitude pulse for 200 ms while applying low suction pressure instead of high suction pulses. If whole cell patch clamp recording is obtained, proceed to option B, otherwise proceed to next step.

ii. If the gigasealed cell is lost during breaking in, or leaky whole cell recording is obtained (indicated, for a typical mouse cortical pyramidal neuron, by a membrane resistance <200 MΩ and current injection required to voltage clamp the patched cell at −65mV of >−200 pA), click **'START OVER'** to stop the current trial and start a new trial from **Step 24**.

Option B) Whole cell patch clamp recording is obtained

i.   Click the **'NEXT'** button in the autopatcher software GUI.

Step 37   **Record the whole cell patched neuron:** Record in voltage or current clamp mode using either the autopatcher software or in commercial software; use the '**External Control**' toggle to switch between these two states if required (Fig. 8). By default the autopatcher holds the whole cell patched cell in voltage clamp mode at −65mV and starts in the '**External Control**' state.

38   **Assess cell quality:** Use the Multiclamp Commander software controls to perform electrode compensation and access resistance compensation as needed. Use the 'Membrane test' function in the data acquisition software (e.g., Clampex) to record the cell parameters such as membrane capacitance, access resistance, membrane resistance, and holding current. At this stage, pipette series resistance, pipette capacitance, and whole cell capacitance (in the case of a voltage clamp recording) may also be compensated using the amplifier control software and the 'Membrane Test' procedure as described in[29]. The cell can then be recorded either in voltage

or current clamp using the data acquisition software. (The recording can also be done entirely in the autopatcher software by switching the left toggle switch in the autopatcher software GUI to **'Autopatcher Control'** and pressing **'Record'**, Fig. 8). The user can switch between current and voltage clamp by switching the right toggle switch with the **'Current Clamp'** and **'Voltage Clamp'** labels. This will send a command to Multiclamp Commander to switch modes. The basic recording and stimulation capability of the software can be extended and customized using the LabVIEW programming environment if of interest (but this is beyond the scope of this paper).

39   **Pipette retraction for recovering biocytin filled cell:** After recording from the cell, press the **'SLOWLY RETRACT PIPETTE'** button in the autopatcher software GUI to retract the pipette in steps of 3 μm every 1 second for up to a total distance of 150 μm followed by a fast retraction to the surface of the brain (Fig. 8). The initial slow retraction allows the gradual resealing of the biocytin-filled cell accompanied by formation of an outside-out patch at the pipette tip. This will preserve the morphology for post experiment processing and reconstruction.

TIMING

The reader should budget an initial setup time for installing and integrating all components of the autopatcher. If all components have been procured at the time of setup, assembling the pipette actuator (**Step 1**) takes 30–60 minutes. The autopatcher control box is the most involved setup step (**Step 2**), and it should take 2–3 days assuming that all the components were procured and circuit boards pre-fabricated. The custom head fixation base and headplates take ~1 day to fabricate (**Steps 3** and **4**). Fabricating the ground electrode and preparing the pipette holder takes ~30 minutes (**Steps 5** and **6**). Once the hardware components have been set up, installing and configuring the software takes 3–4 hours (**Steps 8–11**).

Each experiment commences with the surgical preparation of a mouse, which typically takes 45–60 minutes to complete (**Steps 12–20**). Once the mouse is ready for autopatching, initializing the autopatcher software at the beginning of the experiment takes ~5 minutes (**Steps 21–24**). Installation of the pipette in the autopatcher and positioning it at the craniotomy typically takes 2–3 minutes (**Steps 25–31**) while the autopatching itself takes 3–7 minutes to complete (BOX 2, **Autopatching Steps 1–5**, **Steps 36** and **37**). Time duration of recording from each whole cell patched neuron is determined by the specific experimental goals.

TROUBLESHOOTING

See Table 1 for troubleshooting guidance.

EXPECTED RESULTS

Throughput and yield

The autopatcher can be used to obtain high quality current and voltage clamp data from anesthetized mice (Fig. 9a–d), and recorded neurons can be filled with biocytin for morphological analysis (Fig. 9e). As described previously, under optimized experimental conditions (as described here), one can expect successful whole cell recordings in ~32.9% of the trials on average (n = 24 out of 73 trials)[24], with greater than 60% of the trials yielding good recordings for attempts made within the first hour after opening a fresh craniotomy. Variability in yield might be observed due to variations in the quality of pipettes, the quality of the surgical preparation of the mouse, and the quality of the craniotomy. While the autopatcher has been configured to accept pipettes with resistances between 3–9 MΩ, the generally acceptable range for patch pipette resistances, in our experience best results were obtained using pipettes with resistances between 5–7 MΩ. Patching different neuron types or at different depths or in different species may require different pipette geometries and software settings. The yield of autopatching declines the longer the brain is exposed after the craniotomy is made, as well as with the number of patch attempts made in a particular craniotomy. One strategy to overcome this (if allowed by the experiment) is to attempt autopatching in the more dorsal regions before targeting ventral regions in the pipette descent path. Once cells are autopatched, the cells can be held for an average of ~45 mins with the longest recordings lasting up to three hours, using a quality criterion of resting membrane potential <−50 mV and spike amplitude > 35mV. The throughput of the autopatcher is governed by the time taken to run each trial (3–7 minutes, including the time taken to install the pipette in the setup) and the desired recording duration, which can vary depending on the experiment. There is ongoing work to combine the autopatcher with technologies that can automatically perform craniotomies[29], change pipettes (to enable serial autopatching without human intervention), and potentially to enable parallel computer control of multiple autopatchers with a significant increase in throughput[30].

Quality of recordings

The quality of neuronal recordings obtained with the autopatcher is comparable to that obtained via manual whole cell patch clamping by skilled manual *in vivo* patch clamp practitioners. In our original study[24], we compared the autopatched recordings to those obtained via fully manual patch clamping using commonly used metrics: the access resistance, the holding current required to voltage clamp neurons at −65mV, the resting membrane potential and the recording time. In all these comparisons, no significant difference was observed between autopatched neurons and those obtained via standard *in vivo* patch clamping protocols. These metrics may serve as positive controls for success of the autopatching procedure.

Cell types and morphologies of autopatched neurons

In our original study[24], we analyzed the cell types obtained by the autopatcher. Of the neurons recorded in the cortex and hippocampus in a mouse (91% of all cells patched), typically 68% exhibited regular spiking characteristics, 4% exhibited burst firing patterns, 13% exhibited irregular spike characteristics, 4% exhibited spikes followed by smaller

spikelet events suggestive of backpropagation of action potentials in dendritic recordings, and 2% had spike firing that accelerated. In 9% of the neurons, steady (2s long) current injections over the firing threshold resulted in single action potentials fired, typical of fast adapting neurons. 9% of the recorded cells lacked spiking activity when the membrane potential was depolarized to −30 mV via steadily increasing current injections. Along with this observation and their low cell capacitance characteristics, we concluded that these were glial cells. While not a comprehensive study, these data do illustrate that a variety of cell types can be patch clamped *in vivo* using the autopatcher.

Including 0.4% biocytin (W/V) in the internal pipette solution while autopatching enabled morphological characterization of the recorded cells via standard immuno-histochemical staining protocols. We developed several optimization strategies to obtain high quality morphological reconstructions of autopatched neurons. These include: configuring the autopatcher pipette actuator at an angle (45° to the vertical axis) so as to minimize the number of "ghost stained" (e.g., stained with background levels of biocytin ejected during the approach of the patch pipette) cells in the brain slice containing the recorded neuron, and shortening the duration of recording (10–15 minutes). In our experiments, we were able to recover the morphologies of approximately 75% of the recorded cells based on intensity of staining as well as staining of fine dendritic arbors- which are absent in the "ghost stained" neurons that are found nearby. Of the cells that were morphologically identified, 70% of neurons autopatched in the cortex were pyramidal cells exhibiting apical dendritic structures (Fig. 9c), similar to observations made in other studies[6].

Generalizability of autopatching algorithm

The algorithm used for autopatching was derived in experiments conducted in the cortex of anesthetized mice, but was also useful for obtaining recordings in the hippocampus – exhibiting a degree of generalizability of the algorithm across brain regions. The algorithm is robust enough to allow usage of optic fibers with the patch electrode for simultaneous optogenetic stimulation and autopatching. In a series of experiments, a 200 μm optical fiber was attached to the pipette such that the tip of the fiber was 600 μm lateral from and 500 ± 50 μm above the tip of the electrode tip. This assembly was lowered into the brain using the autopatcher to obtain whole cell patch recordings and subsequently measured photo-evoked hyperpolarization of motor cortex neurons expressing the red-shifted optogenetic silencer Jaws[26] (Fig. 9g) and photo-evoked spikes from neurons expressing channelrhodopsin-2 in a Thy1-ChR2 transgenic mouse[31] (Fig. 9h). Coupling of other devices to the autopatcher setup[32] may enable the integration of the autopatcher into experiments involving extracellular recording, pharmacological infusion and other neuroscience strategies of importance. As a final note, the protocol described above has been tried and tested in anesthetized mice. We have also successfully utilized the autopatcher to obtain whole cell patch recordings in awake headfixed animals (**Fig. f**), both in a fully immobilized setting[11, 33] as well as from headfixed animals on a spherical virtual reality treadmill[14, 34].

Supplementary Material

Refer to Web version on PubMed Central for supplementary material.

Acknowledgments

References

1. Bruno RM, Sakmann B. Cortex is driven by weak but synchronously active thalamocortical synapses. Science. 2006; 312:1622–1627. [PubMed: 16778049]

2. Arenz A, Silver RA, Schaefer AT, Margrie TW. The contribution of single synapses to sensory representation in vivo. Science. 2008; 321:977–980. [PubMed: 18703744]

3. Brecht M, Schneider M, Sakmann B, Margrie TW. Whisker movements evoked by stimulation of single pyramidal cells in rat motor cortex. Nature. 2004; 427:704–710. [PubMed: 14973477]

4. Chadderton P, Margrie TW, Hausser M. Integration of quanta in cerebellar granule cells during sensory processing. Nature. 2004; 428:856–860. [PubMed: 15103377]

5. Eberwine J, et al. Analysis of gene expression in single live neurons. Proc Natl Acad Sci U S A. 1992; 89:3010–3014. [PubMed: 1557406]

6. Rancz EA, et al. Transfection via whole-cell recording in vivo: bridging single-cell physiology, genetics and connectomics. Nat Neurosci. 2011; 14:527–532. [PubMed: 21336272]

7. Margrie TW, Brecht M, Sakmann B. In vivo, low-resistance, whole-cell recordings from neurons in the anaesthetized and awake mammalian brain. Pflugers Arch. 2002; 444:491–498. [PubMed: 12136268]

8. Chadderton P, Agapiou JP, McAlpine D, Margrie TW. The synaptic representation of sound source location in auditory cortex. The Journal of neuroscience : the official journal of the Society for Neuroscience. 2009; 29:14127–14135. [PubMed: 19906961]

9. Chadderton P, Margrie TW, Hausser M. Integration of quanta in cerebellar granule cells during sensory processing. Nature. 2004; 428:856–860. [PubMed: 15103377]

10. Crochet S, Petersen CCH. Correlating whisker behavior with membrane potential in barrel cortex of awake mice. Nat Neurosci. 2006; 9:608–610. [PubMed: 16617340]

11. Crochet S, Poulet JF, Kremer Y, Petersen CC. Synaptic mechanisms underlying sparse coding of active touch. Neuron. 2011; 69:1160–1175. [PubMed: 21435560]

12. Gentet LJ, Avermann M, Matyas F, Staiger JF, Petersen CC. Membrane potential dynamics of GABAergic neurons in the barrel cortex of behaving mice. Neuron. 2010; 65:422–435. [PubMed: 20159454]

13. Gentet LJ, et al. Unique functional properties of somatostatin-expressing GABAergic neurons in mouse barrel cortex. Nat Neurosci. 2012; 15:607–612. [PubMed: 22366760]

14. Harvey CD, Collman F, Dombeck DA, Tank DW. Intracellular dynamics of hippocampal place cells during virtual navigation. Nature. 2009; 461:941–946. [PubMed: 19829374]

15. Hromadka T, DeWeese MR, Zador AM. Sparse representation of sounds in the unanesthetized auditory cortex. Plos Biol. 2008; 6:124–137.

16. Schaefer AT, Margrie TW. Spatiotemporal representations in the olfactory system. Trends Neurosci. 2007; 30:92–100. [PubMed: 17224191]

17. Kitamura K, Judkewitz B, Kano M, Denk W, Hausser M. Targeted patch-clamp recordings and single-cell electroporation of unlabeled neurons in vivo. Nat Meth. 2008; 5:61–67.

18. Komai S, Denk W, Osten P, Brecht M, Margrie TW. Two-photon targeted patching (TPTP) in vivo. Nat Protoc. 2006; 1:647–652. [PubMed: 17406293]

19. Margrie TW, et al. Targeted whole-cell recordings in the mammalian brain in vivo. Neuron. 2003; 39:911–918. [PubMed: 12971892]

20. Lee AK, Epsztein J, Brecht M. Head-anchored whole-cell recordings in freely moving rats. Nat Protocols. 2009; 4:385–392. [PubMed: 19247288]

21. Lee AK, Manns ID, Sakmann B, Brecht M. Whole-cell recordings in freely moving rats. Neuron. 2006; 51:399–407. [PubMed: 16908406]

22. Lee D, Lin BJ, Lee AK. Hippocampal Place Fields Emerge upon Single-Cell Manipulation of Excitability During Behavior. Science. 2012; 337:849–853. [PubMed: 22904011]

23. Long MA, Jin DZ, Fee MS. Support for a synaptic chain model of neuronal sequence generation. Nature. 2010; 468:394–399. [PubMed: 20972420]

24. Kodandaramaiah SB, Franzesi GT, Chow BY, Boyden ES, Forest CR. Automated whole-cell patch-clamp electrophysiology of neurons in vivo. Nat Meth. 2012; 9:585–587.

25. DeWeese MR. Whole-cell recording in vivo. Curr Protoc Neurosci. 2007:22. Chapter 6, Unit 6. [PubMed: 18428661]

26. Chuong AS, et al. Noninvasive optical inhibition with a red-shifted microbial rhodopsin. Nat Neurosci. 2014; 17:1123–1129. [PubMed: 24997763]

27. Margrie TW, Brecht M, Sakmann B. In vivo, low-resistance, whole-cell recordings from neurons in the anaesthetized and awake mammalian brain. Pflugers Arch. 2002; 444:491–498. [PubMed: 12136268]

28. Schramm AE, Marinazzo D, Gener T, Graham LJ. The Touch and Zap Method for <italic>In Vivo</italic> Whole-Cell Patch Recording of Intrinsic and Visual Responses of Cortical Neurons and Glial Cells. PLoS One. 2014; 9:e97310. [PubMed: 24875855]

29. Pak N, et al. Closed-loop, ultraprecise, automated craniotomies. Journal of neurophysiology. 2015; 113:3943–3953. [PubMed: 25855700]

30. Kodandaramaiah SB, Boyden ES, Forest CR. In vivo robotics: the automation of neuroscience and other intact-system biological fields. Annals of the New York Academy of Sciences. 2013; 1305:63–71. [PubMed: 23841584]

31. Arenkiel BR, et al. In Vivo Light-Induced Activation of Neural Circuitry in Transgenic Mice Expressing Channelrhodopsin-2. Neuron. 2007; 54:205–218. [PubMed: 17442243]

32. Harrison RR, et al. Microchip amplifier for in vitro, in vivo, and automated whole-cell patch-clamp recording. 2014

33. Poulet JFA, Fernandez LMJ, Crochet S, Petersen CCH. Thalamic control of cortical states. Nat Neurosci. 2012; 15:370–372. [PubMed: 22267163]

34. Polack PO, Friedman J, Golshani P. Cellular mechanisms of brain state-dependent gain modulation in visual cortex. Nat Neurosci. 2013; 16:1331–1339. [PubMed: 23872595]

35. Plant, TD.; Eilers, J.; Konnerth, A. Patch-Clamp Applications and Protocols. Boulton, A.; Baker, G.; Walz, W., editors. Vol. 26. Humana Press; 1995. p. 233-258.

Author Manuscript

BOX 1

The patch pipette is an important component of the autopatcher and can have significant effect on the yield and quality of recordings obtained by the autopatcher. In our laboratory, we have consistently obtained high quality and high yield autopatched recordings using pipettes with certain geometrical characteristics. Our pipettes typically exhibit tip diameters of 0.8 – 0.9 μm (corresponding to a range of 5 to 7 MΩresistance, Fig. 3). The general taper of the pipette leading up to the tip has a convex curvature. Pipettes with concave tapers typically have high variability in their resistances and may give variable results while autopatching. Finally, a broad cone angle assists in obtaining stable gigaseals and low access resistance when the whole cell configuration is obtained.

To optimize the pipette geometry, a good starting point is to follow the pipette puller's instruction manual to program it to pull pipettes which have resistances in the range of 3–9 MΩ. Then the velocity and heat settings (in the case of a Flaming Brown puller) can be adjusted to obtain pipettes of the desired resistance range of 5–7 MΩ. Typically higher velocity and heat settings result in pipettes with longer tapers and smaller tip diameters with corresponding increases in pipette resistance. Refer to the pipette puller's user manual for instruction on adjusting pulling parameters to obtain pipette with optimum geometries. Further, the performance of the electronics and heating components in the pipette puller can drift over a period of time. To account for these drifts, it is recommended that the puller is switched on well in advance (or even left on continuously during days of experimentation) so the electronic circuitry is at steady state. Capillary glass with the same dimensions from two different vendors (or even from one batch to the other) can behave very differently when pulled using the same program due to differing melting points and geometrical tolerances. Thus the puller needs to be programmed for each type of glass capillary being used. As a final note, it is important to pull pipettes within a few hours before an autopatching experiment. It is not advisable to use pipettes that have been stored for longer time durations, even if they have been kept in sealed airtight containers, since the surface properties may change due to dust in the air, significantly increasing the chance that the pipette tip will be clogged.

BOX 2

AUTOPATCHING

Autopatching Step 1: Checking the pipette outside the brain: The autopatcher first checks if the pipette is suitable for autopatching (Fig. 1a.ii) before insertion into the brain. It measures the pipette resistance in one second intervals for twenty seconds and displays these values in the **'Initial Pipette Resistance Assessment'** graph in the autopatcher software GUI (Fig. 5). At the end of twenty seconds, the average of the measured pipette resistances is displayed in the '**Average resistance during initial pipette assessment (M-Ohms)'** report box, and the variance in measured pipette resistances is displayed in the **'Resistance variation during initial pipette assessment (M-ohms)'** report box (Fig. 5). At the end of this check, one of two cases can occur:

i.   Pipette is suitable for autopatching: The autopatcher will then proceed to **Autopatching Step 2**.

ii. Pipette is unsuitable for autopatching: If the pipette resistance is not within the range of 3–9 MΩ or the variation in the resistance measurements is greater than 50 KΩ, the autopatcher software GUI will display a pop-up dialog box instructing the experimenter to install a new pipette in the autopatcher for the next trial. (Advanced users desiring to push autopatching beyond the current specifications can of course modify the software to alter these defaults, e.g. if very fine pipettes are being used to attempt dendritic patching, but that is beyond the scope of this paper.) See **Step 32** in the main protocol for required user intervention.

Autopatching Step 2: Regional pipette localization: The autopatcher lowers the pipette to the depth specified by the experimenter (**Step 24**), and waits one second before lowering the pressure inside the pipette from high positive pressure to low positive pressure (Fig. 1a.iii). It waits five seconds and then measures the resistance of the pipette at this depth. This resistance value is displayed in the **'Resistance at beginning of neuron hunt (M-Ohms)'** report box in the autopatcher software GUI (Fig. 5). At this point one of three cases will occur:

i.   The autopatcher detects no clogging or breakage of pipette tip during the descent to depth: In this case, the autopatcher proceeds to **Autopatching Step 3 – neuron hunting** (Fig. 1a.iv). Panel 4 of the autopatcher software GUI automatically switches to 'Neuron Hunt' (Fig. 6a).

ii. The autopatcher detects a clogging/fouling of pipette tip during the descent to depth (pipette resistance measured after lowering the pipette to depth is **greater** than pipette resistance measured outside the brain by more than 0.35 MΩ[24]): In this case, the autopatcher retracts the pipette out of the brain and displays a pop-up dialog box in the autopatcher software GUI indicating that the pipette tip is clogged/fouled and instructs the experimenter to replace the

pipette for the next trial. See **Step 33** in the main protocol for required user intervention.

iii. The autopatcher detects a breakage of the pipette tip during the descent to depth: (pipette resistance measured after lowering the pipette to depth is **lower** than pipette resistance measured outside the brain by more than 2.0 MΩ): In this case, the autopatcher will immediately halt positive pressure, retract the pipette out of the brain, and display a pop-up dialog box in the autopatcher software GUI indicating that the pipette tip is broken and instructs the experimenter to replace the pipette for the next trial.

Autopatching Step 3: Neuron hunting: The autopatcher moves the pipette down by 2μm every 2s and measures the pipette resistance. These resistance values at each position are logged and displayed in the **"NEURON HUNTING RESISTANCE MONITOR"** graph during the neuron hunting process (Fig. 6a). Contact with a neuron is detected when resistance increases monotonically over three steps and when the total increase is larger than the neuron detection threshold set in the **'Neuron detection threshold (M-Ohms)'** numerical entry box (the default value is 0.25 MΩ, as described in ref.[24]). A representative screen shot of a resistance trace recorded during a successful neuron hunting attempt is shown in Figure 6b.

Autopatching Step 4: Gigasealing: If a neuron is detected during neuron hunting, the advancement of the pipette is stopped and the autopatcher commences a gigasealing attempt (Fig. 7a and b). The pipette resistance is now measured in intervals of 500ms and displayed in the **'GIGASEALING RESISTANCE MONITOR'** graph. After the pipette resistance is measured for 10s, one of two cases will occur:

i. The autopatcher confirms that a neuron has been contacted (pipette resistance stays at the elevated value in the 10 seconds after the neuron was detected in **Autopatching Step 3**): In this case, the autopatcher proceeds to the next stage of gigasealing and switches to atmospheric pressure after 10 seconds. At the same moment the pressure is switched, the holding voltage is changed to −30 mV and ramps down to −70 mV. Additional detail about the algorithm can be found in the original paper[24]. The pipette resistances are plotted in the **'GIGASEALING RESISTANCE MONITOR'** graph in the autopatcher software GUI (Fig. 7a). A representative trace of resistance measurements during a successful gigasealing attempt is shown in Fig. 7b. Successful gigaseals (seal resistance >1000 MΩ typically form in the first 30–90 seconds of gigasealing, and occur in about 60% of the autopatcher trials where the neuron hunting stage was reached.

ii. The autopatcher detects a false positive in the neuron detection (pipette resistance goes back to the baseline value measured before neuron detection in **Autopatching Step 3**, detected by comparing the average resistance measured in the last 4 seconds to the average resistance measurement in the first 4 seconds of this step): In this case, the autopatcher reverts back to neuron

hunting (**Autopatching Step 3**) until the criterion for neuron detection are met again.

Autopatching Step 5: Confirming gigaseal formation: 60s after the commencement of gigasealing, the autopatcher checks if a gigaseal has been successfully formed. One of two cases will then occur:

i. Gigaseal has been obtained (seal resistance >1000 MΩ, Fig. 1a.vi and Fig 7b: The autopatcher displays a pop-up dialog box indicating a successful gigaseal has been formed. Proceed to **Step 34**.

ii. Gigaseal has not been obtained (seal resistance <1000 MΩ): The autopatcher continues measuring the seal resistance every 500ms and updates the **'GIGASEALING RESISTANCE MONITOR'** graph. It is highly unlikely that a gigaseal will form if the seal resistance is less than 100 MΩ after 60s of gigasealing operation. Proceed to **Step 34**.
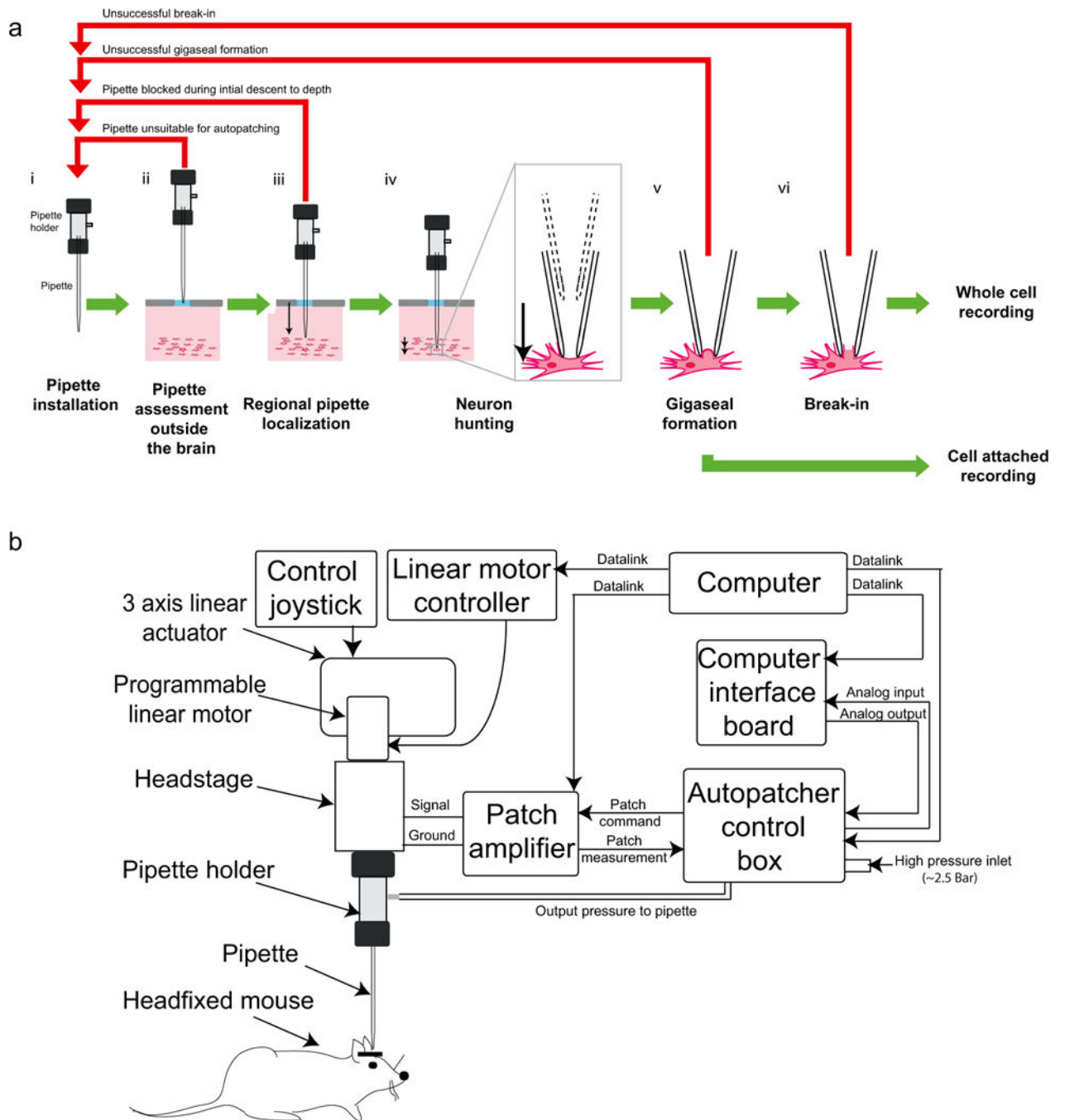
FIGURE 1. The autopatcher – a robot for automated whole cell patch clamp recordings *in vivo*: overview of algorithm and schematic

(**a**) The algorithm for autopatching (adapted from Kodandaramaiah et al 2012): The six stages of obtaining whole cell patch clamp recordings in vivo include: (**i**) all the manual steps (**Steps 12–31**: installing a pipette, software initialization, etc.) that need to be performed after which the autopatcher will programmatically perform **Steps 24–31 (ii)** an initial assessment of the resistance of the patch pipette to eliminate unsuitable pipettes (BOX 2, **Autopatching Step 1**), (**iii**) lowering of the patch pipette to the region of interest followed

by a second assessment of pipette tip fidelity (BOX 2, **Autopatching Step 2**), (iv) the neuron hunting stage during which the autopatcher scans for neurons (BOX 2, **Autopatching Step 3**), (v) attempting gigasealing by modulating the pressure inside the pipette and pipette voltage after contact with a cell has been established (BOX 2, **Autopatching Step 4–5**), and (**vi**) the break-in stage during which pulses of high negative pressure are applied to achieve the whole cell patch clamp state (**Step 36**). Some fraction of the autopatcher trials result in end points other than acquisition of whole cell patched or cell attached recordings. Such instances are highlighted with the red arrows and explained in the corresponding steps in the protocol. (**b**) Schematic of the autopatcher system capable of performing the autopatching algorithm (adapted from Kodandaramaiah et al 2012): The system consists of a conventional *in vivo* patch setup (i.e., pipette, headstage, 3 axis linear actuator, patch amplifier and computer), equipped with a few additional modules: a programmable linear motor and a custom control box for data acquisition to enable closed-loop control of the motor based upon a series of pipette resistance measurements. The control box also performs closed-loop pneumatic pressure control of the patch pipette. (a) and (b) adapted from Kodandaramaiah et al 2012[24].
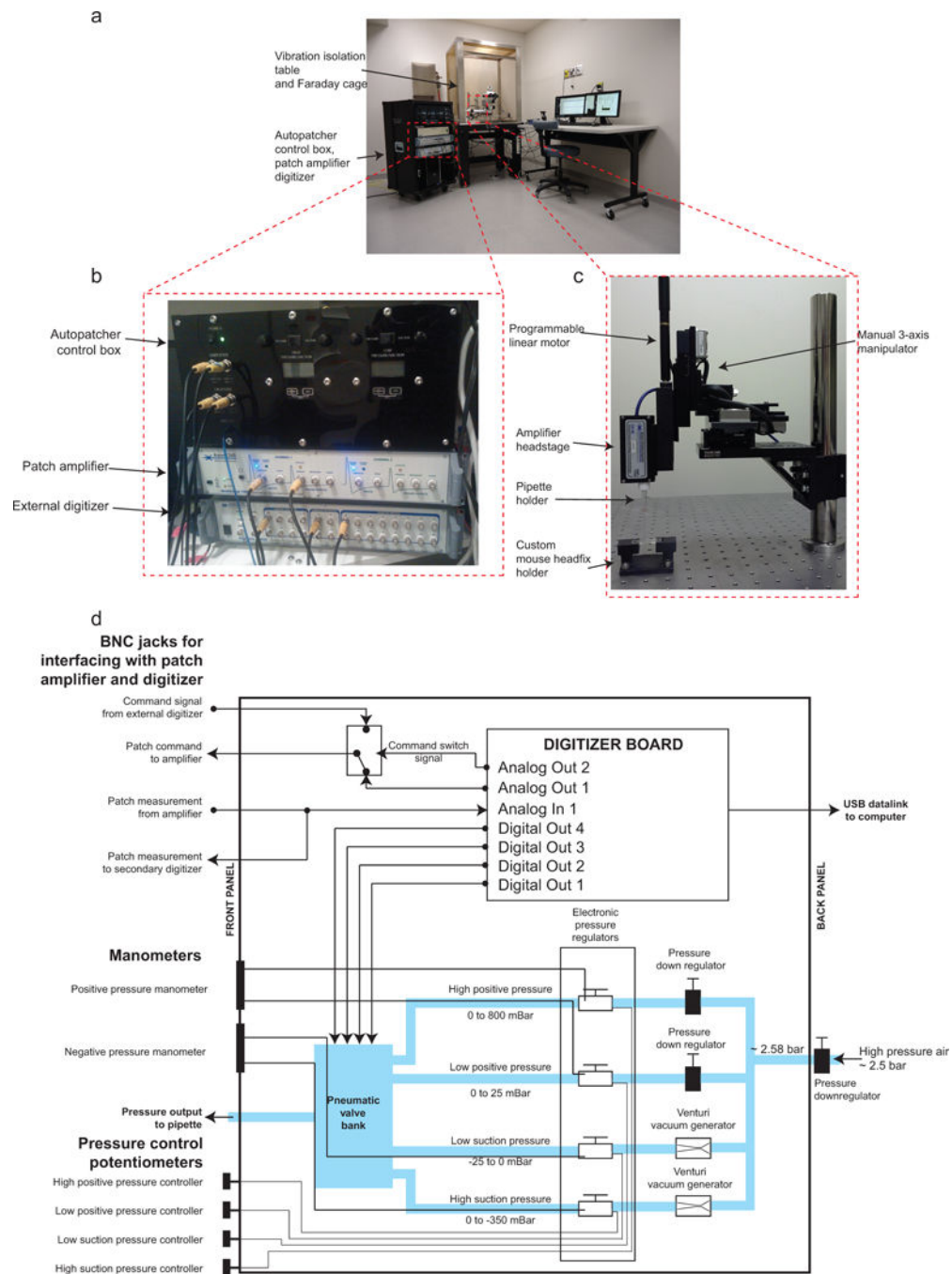
FIGURE 2. The autopatcher: equipment photographs

(**a**) Photograph of the autopatcher showing the general layout of major equipment. (**b**) Photograph focusing on the autopatcher control box and its interface with the patch amplifier and external digitizer. (**c**) Photograph focusing on the pipette actuator assembly. (**d**) Schematic of the autopatcher control box. A central digitizer board equipped with analog inputs, as well as analog and digital outputs, in the autopatcher control box sends command voltage signals to the patch amplifier and reads the patch measurements from the amplifier output. Digital outputs on the same board are sent to a bank of pneumatic valves (described

in ref[7] and in the assembly manual '**Autopatcher control box assembly manual.pdf**' in Supplementary Data 4) to switch between different pressure states during autopatcher operation. The four pressures are generated by downregulating a compressed air source of ~2580 mBar using manual and electronic pressure regulators whose outputs can be controlled using knobs on the front panel of the control box (potentiometers in the lower left hand corner). Vacuum pressures are generated using Venturi tube vacuum generators also installed inside the autopatcher control box.
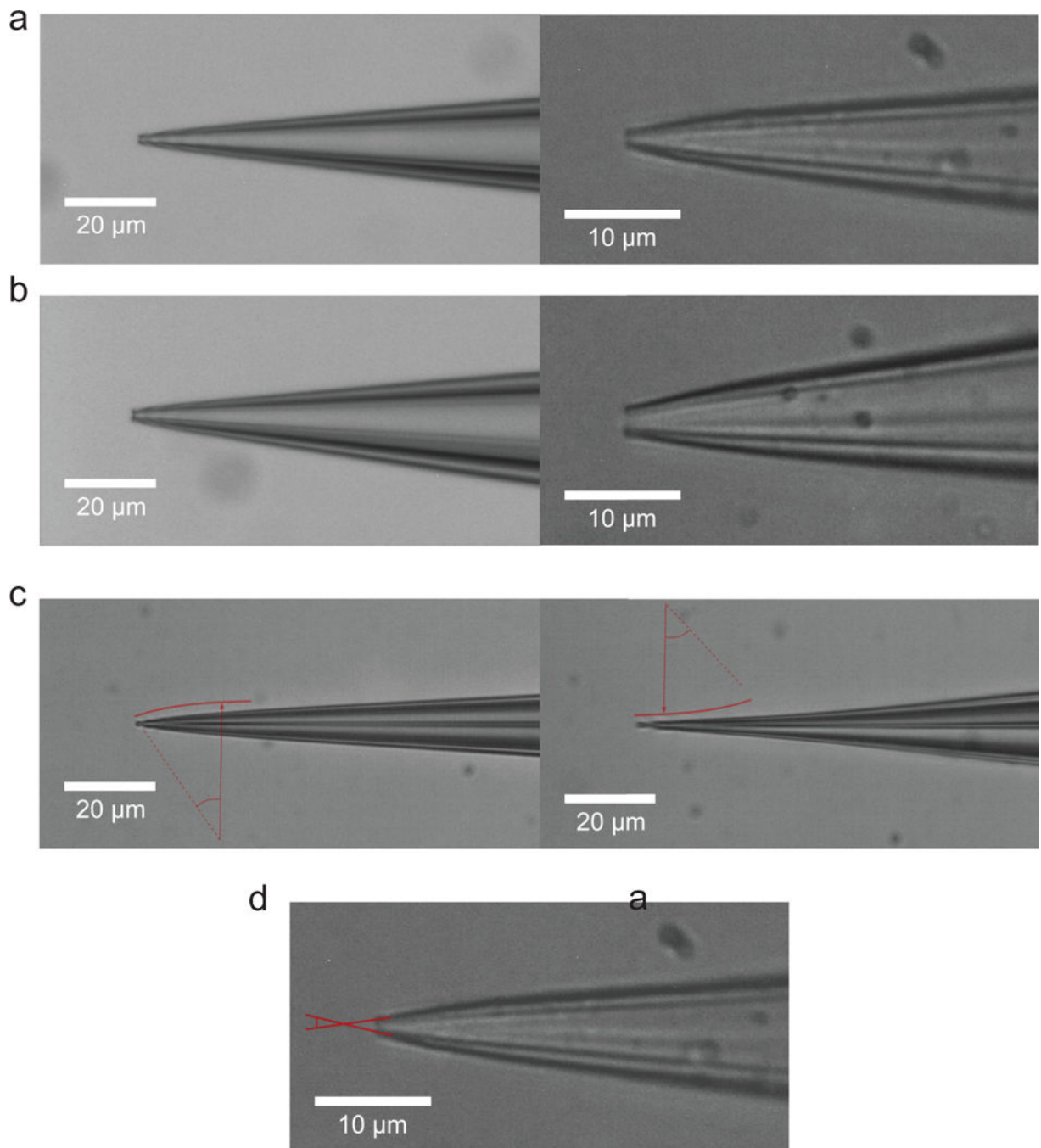
FIGURE 3. Optimum pipettes used for autopatching
(a) Photomicrographs of an ideal patch pipette pulled using a Flaming Brown pipette puller focusing on the pipette tip with 0.9 μm tip diameter (6.2 MΩ resistance) visualized with a 40× magnification objective (left) and 100× water immersion objective (right) in comparison to **(b)** a patch pipette with 1.5 μm tip diameter (3.3 MΩ resistance) visualized with a 40× magnification objective (left) and 100× water immersion objective (right). **(c)** Comparison of a convex tapered pipette which is ideal for autopatching (left) vs. concave tapered pipettes (right) and **(d)** illustration of an ideal patch pipette exhibiting broad cone angle. Larger tip

angles, as measured in the image at the very tip of the pipette, are ideal for rapid gigasealing, stable recordings, and easier break-in attempts.
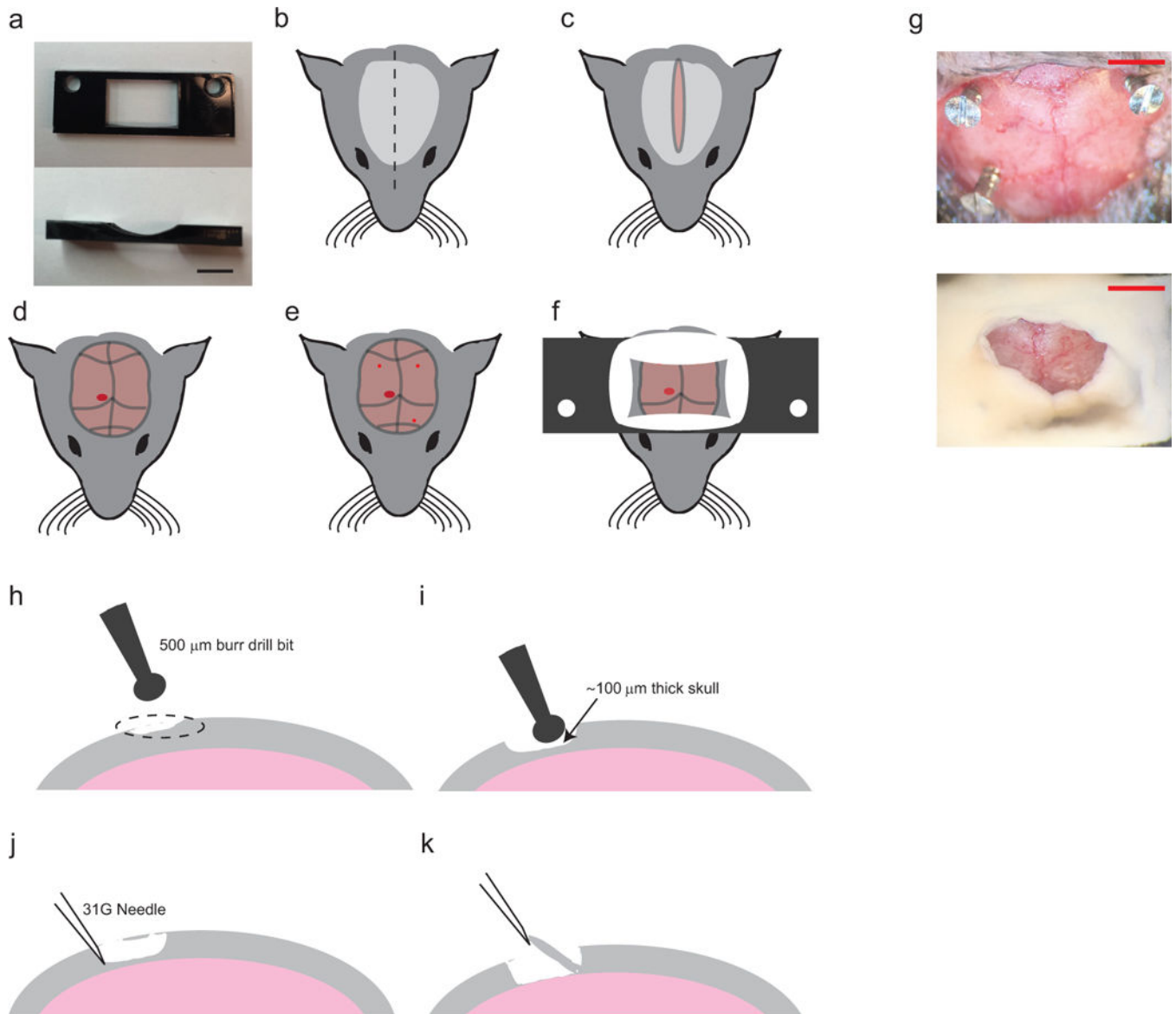
FIGURE 4. Surgical procedure for headplate implantation
(a) top (left) and side (right) views of the Delrin headplate to be affixed to the skull for head stabilization during autopatching. Scale bar indicates 5 mm. **(b–f)** Preparation and surgery of the anesthetized mouse after administering approved anesthetic, followed by shaving and sterilizing the scalp. First perform longitudinal incision of the scalp (b, c) to expose the skull **(d)**. Clear the skull further around the desired recording region, **(d; red circle)**. Using a burr drill bit, drill three anchor holes (~500 μm diameter, *three small red circles*; e) and implant skull screws. Finally implant the headplate by applying freshly mixed dental acrylic cement around the skull screws and around the periphery of the headplate window **(f). (g)** Photographs of the mouse skull after implantation of the skull screws (top) and after implantation of the headplate (bottom). Scale bars indicate ~2mm **(h–k)** Illustration of the craniotomy procedure. Identify the desired craniotomy location (h), thin down a 1–2 mm wide pit at the desired craniotomy location until the remaining bone is ~100 μm thick (i),

carefully dislodge the flaky bone tissue with a tip of a needle (j), and lift off the bone tissue and clear any remaining bone fragments (k). **CAUTION:** All animal use should comply with institutional and federal regulations.
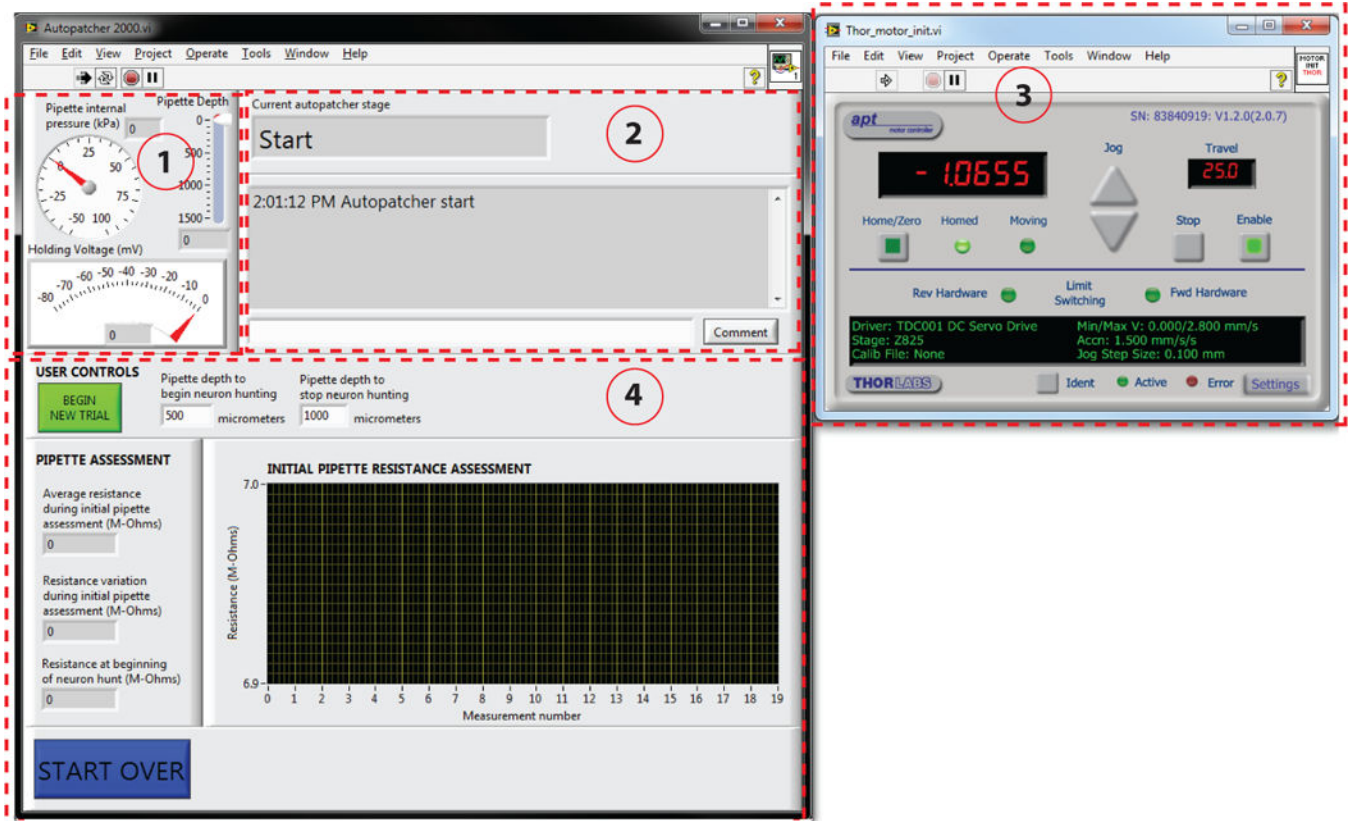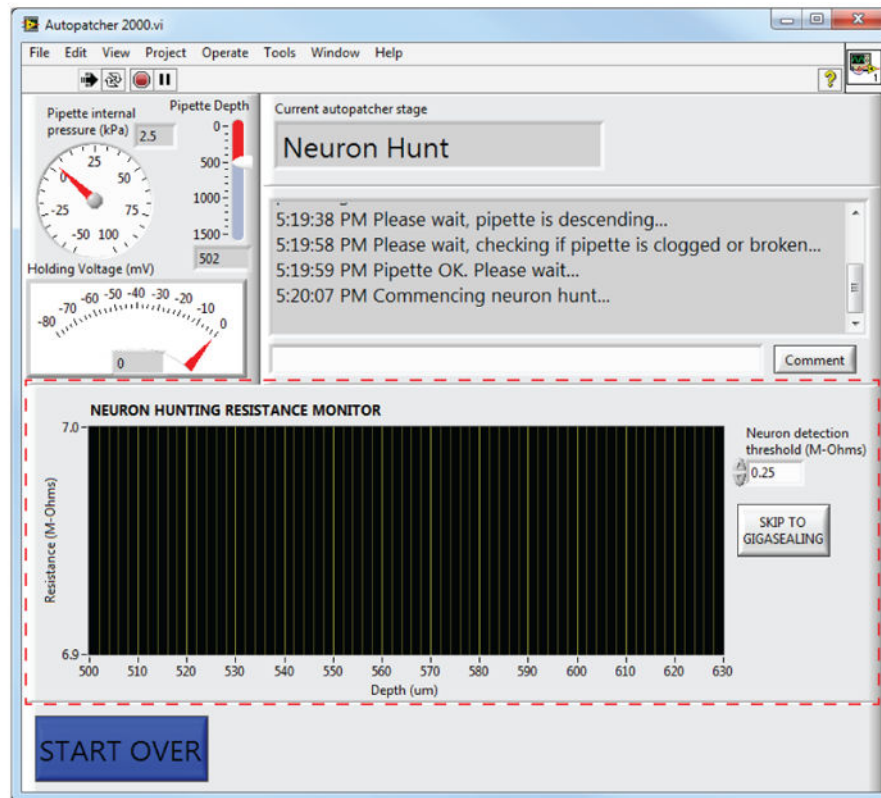
FIGURE 5. Autopatcher software graphical user interface (GUI)
Red dotted lines outline different panels of the GUI. **Panel (1):** Pipette status indicators that display the instantaneous pipette position (in μm) from surface of the brain, pressure applied to the pipette (in kPa), and the holding voltage (in mV) applied to the pipette during autopatcher operation. **Panel (2):** Text indicators that display the current status of the autopatcher trial, and a log of all autopatching trials attempted during an experiment, as well as an entry box where the experimenter can log comments. **Panel (3):** Includes control elements that allow the experimenter to control the programmable motor. This displays the absolute position of the pipette in motor coordinates. **Panel (4):** The interactive elements displayed in this panel depend on the stage of autopatching, and include methods for setting the beginning and ending depth ranges within which the autopatcher will scan for neurons, amongst other things (see Figs. 6 and 7 and Supplementary Video 1 to see how this box changes throughout the protocol).
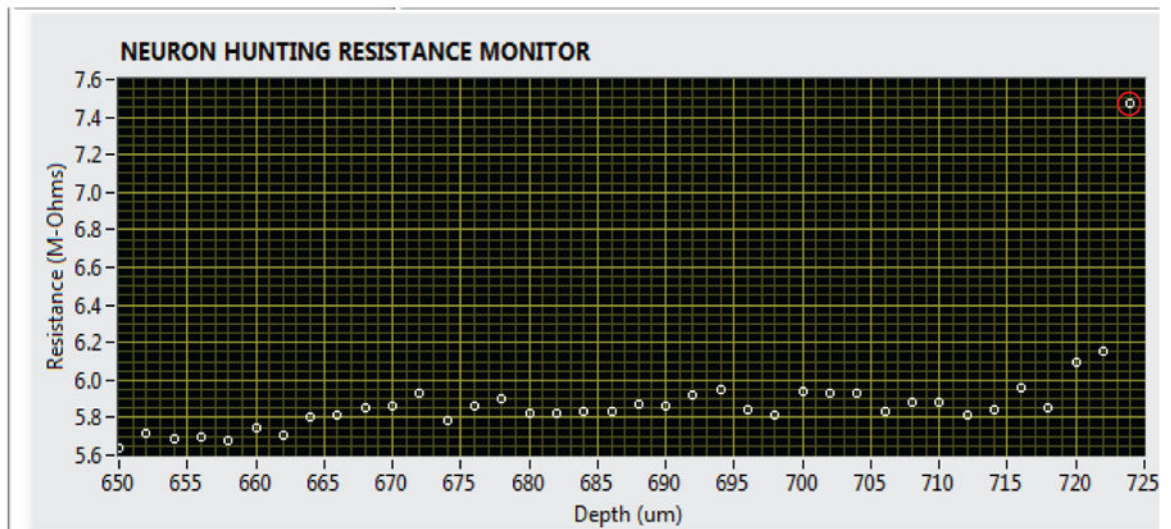
FIGURE 6. Autopatcher software graphical user interface: neuron hunting
(a) The autopatcher software GUI displayed during the neuron hunting stage (BOX 2,
Autopatching Step 3 in the protocol) of autopatching: red dotted lines highlight the
indicators and user controls in **Panel 4** of Figure 5 that can be accessed during this stage.
The measured resistances after each step taken during neuron hunting are plotted on the
"NEURON HUNTING RESISTANCE MONITOR" graph. The **'SKIP TO
GIGASEALING'** button allows the experimenter to override the neuron detection
algorithm of the autopatcher and proceed to the gigasealing stage. The resistance threshold

the algorithm uses to switch from neuron hunting to gigasealing mode can be changed as needed in the '**Neuron detection threshold (M-Ohms)**' numerical entry box (default, 0.25 $M\Omega^{1}$). **(b)** Representative screen shot of the **"NEURON HUNTING RESISTANCE MONITOR"** graph displaying the resistance measurements logged during a successful trial resulting in a whole cell patch recording. The autopatcher initially lowered the pipette to a depth of 650 μm and scanned to a depth of 720 μm before encountering a neuron as indicated by the monotonic increase in pipette resistance in the last data points.
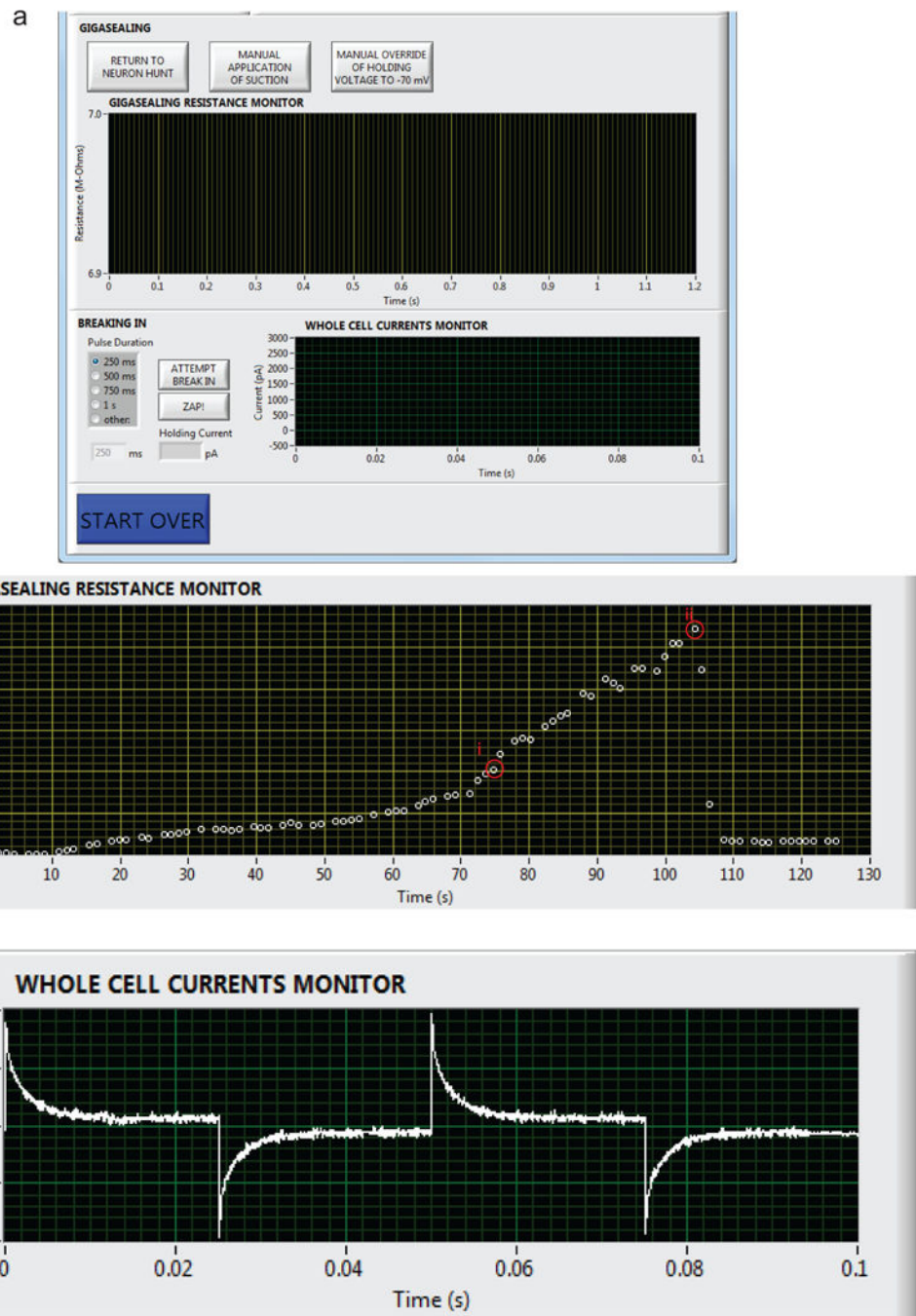
FIGURE 7. Autopatcher software graphical user interface: gigasealing and break-in
(a) Panel 4 in Figure 5, now showing the autopatcher software GUI displayed during the
gigasealing and break-in stages of autopatching (BOX 2, Autopatching **Steps 4 and 5, Step
34 and 35**). The **'GIGASEALING RESISTANCE MONITOR'** graph displays the
recorded seal resistances during a gigasealing attempt. The '**RETURN TO NEURON
HUNT**' button allows the experimenter to override the autopatcher operation and return to
the neuron hunting stage of autopatching. The '**MANUAL APPLICATION OF
SUCTION**' button allows the experimenter to override the autopatcher algorithm's negative

pressure application to manually apply additional negative pressure at any time during gigasealing and allows exploration of alternate strategies for gigasealing used in *in vivo* and *in vitro* slice patching[25, 35]. Once a successful gigaseal is formed, break-in can be attempted by using the **'ATTEMPT BREAK IN'** button, which causes the autopatcher to apply pulses of negative pressure of selected time duration. Alternatively, break-in can be attempted by applying voltage pulses using the **'ZAP!'** button. The '**WHOLE CELL CURRENTS MONITOR**' graph displays the currents in response to injected voltage square waves after a break-in attempt so the user can assess whether it has achieved the whole cell configuration. **(b)** Screen capture of seal resistance measurements displayed in the **'GIGASEALING RESISTANCES MONITOR'** graph in the autopatcher software GUI during a successful gigasealing attempt. A GΩ seal was obtained at time point **(i)**. The '**ATTEMPT BREAK IN**' button was utilized by the experimenter at t = 105 s to break into the cell. Whole cell configuration was obtained at time point **(ii). (c)** Illustration of currents measured and displayed in the '**WHOLE CELL CURRENTS MONITOR**' graph in the autopatcher software GUI after a successful break-in attempt resulting in a whole cell patched neuron.
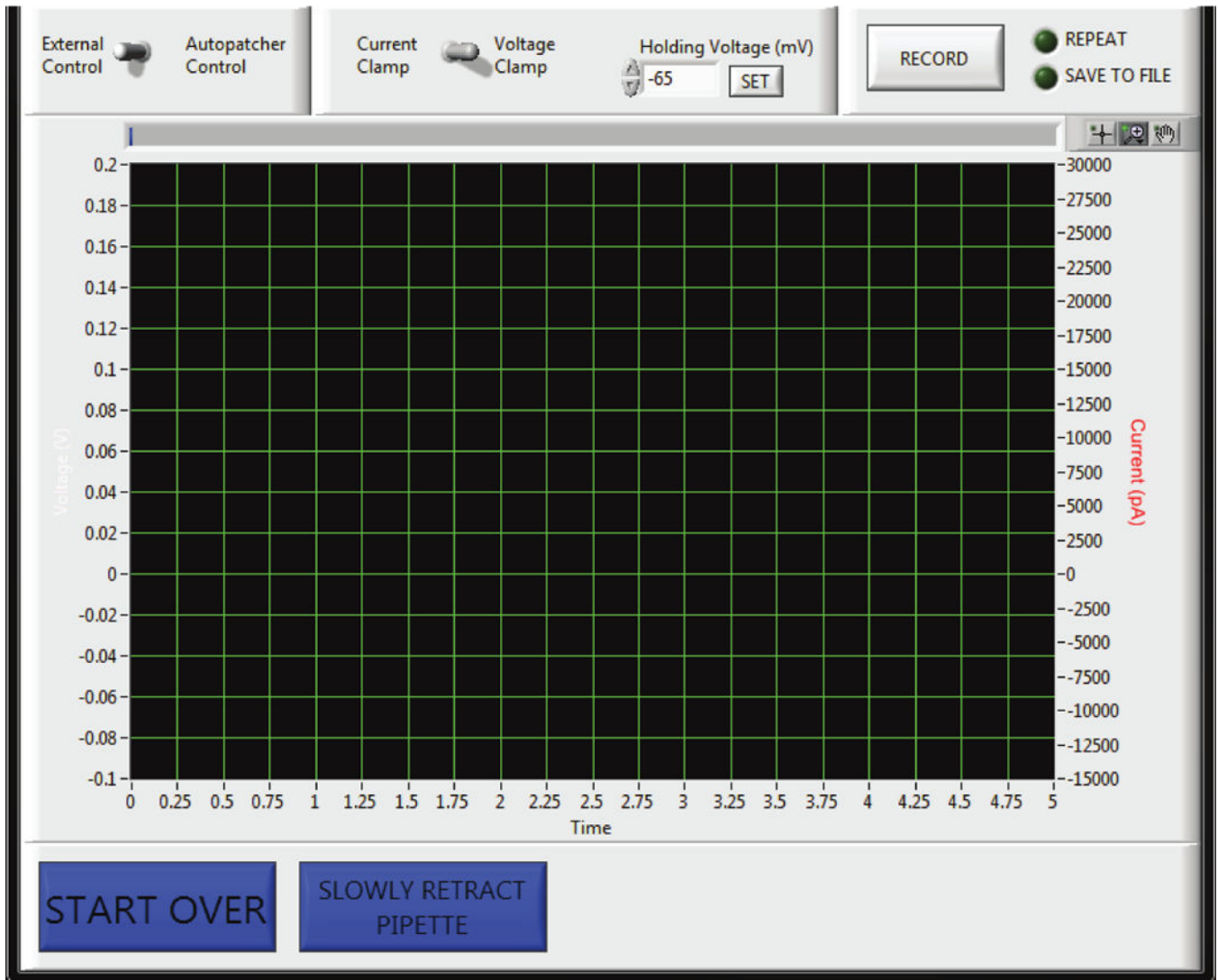
FIGURE 8. Autopatcher software graphical user interface: recording

(a) Panel 4 in Figure 5, now showing the autopatcher software GUI displayed during the recording stage after autopatching (**Step 37–39**). A toggle switch allows the user to use either the built-in data acquisition feature under '**Autopatcher Control**' or to use an external data acquisition software under '**External Control**'. If the '**Autopatcher Control**' option is used, a second toggle switch allows the user to switch between voltage clamp and current clamp mode. A numerical entry box allows the user to set the holding voltage (in mV, if recording in voltage clamp mode) or holding current (in pA, if recording in current clamp mode). When the '**RECORD**' button is pressured, the measured currents (if recording in voltage clamp mode), or measured voltage (if recording in current clamp mode), are displayed in the graph indicator. The '**REPEAT**' button can be used to acquire data continuously, and the '**SAVE TO FILE**' button saves the file to disk. Pressing the '**START OVER**' button ends the recording and the autopatcher will retract the patch pipette back to the surface in one quick step lasting ~500 ms for pipette retrieval and replacement to start a new trial. To recover the morphology of the recorded cell, biocytin filling is attempted by

pressing the '**SLOWLY RETRACT PIPETTE**' button, which will result in the autopatcher withdrawing the patch pipette back to the surface of the brain at a rate of 3 μm/s.
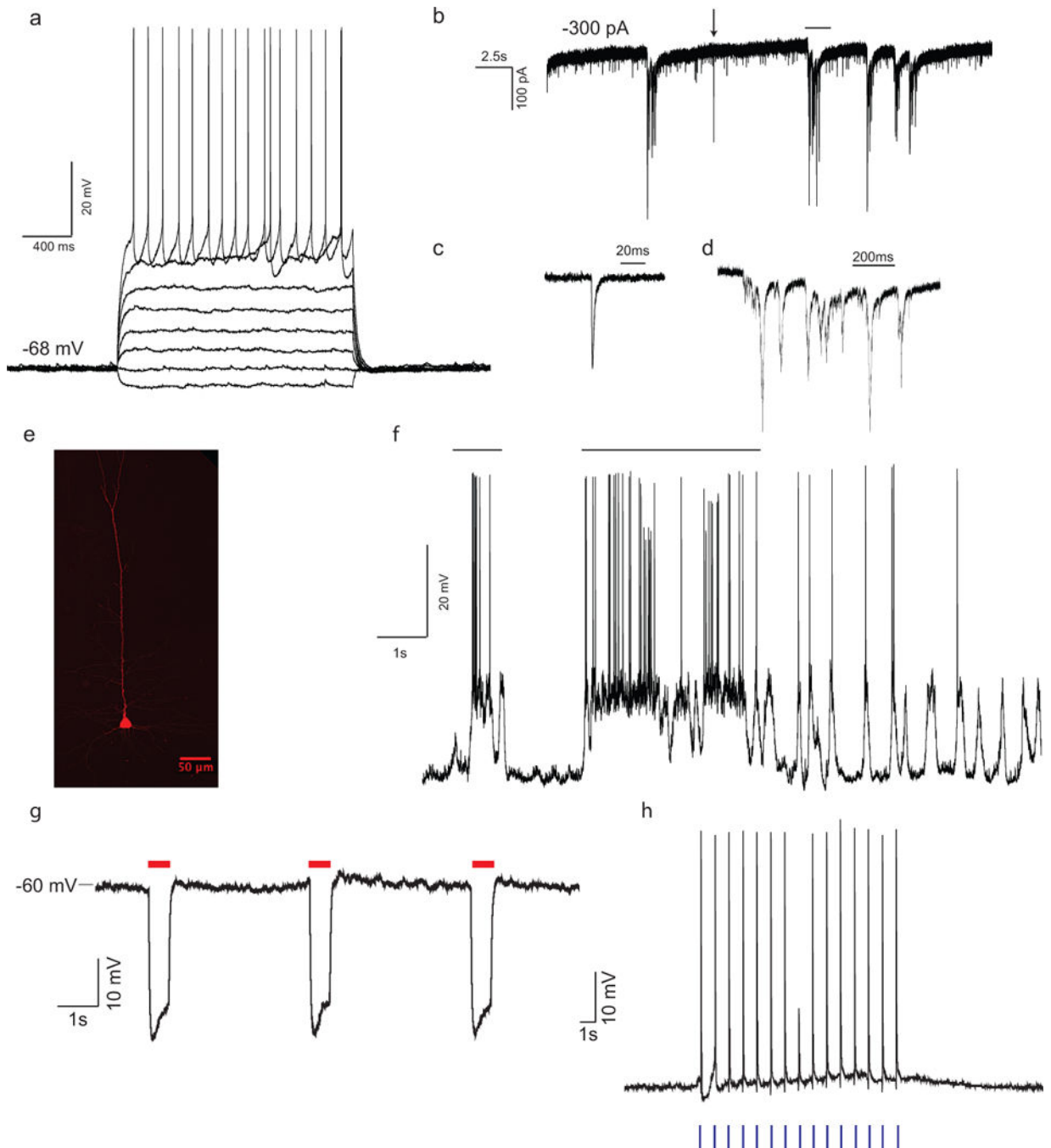
FIGURE 9. Example data acquired by the autopatcher
(a) Current clamp recording from autopatched cortical neuron during current injection (2s long pulses of −30, 0, +30, +60, +90, +120, +150 and +180 pA current injection). Access resistance, 44 MΩ; input resistance, 66 MΩ; depth of cell 442 μm below surface of the brain. (b–d) Voltage clamp recordings from an autopatched cortical neuron clamped at −80 mV (b) showing spontaneous excitatory post-synaptic potentials (EPSCs), (c) zooming in on single synaptic event indicated by black arrow in (b), and (d) zooming in synaptic barrage event indicated by black bar in (b). Access resistance 23 MΩ; input resistance 124 MΩ; depth of

cell 544 μm from surface of the brain. **(e)** Biocytin fill of the autopatched cortical pyramidal neuron recorded in **(a). (f)** Autopatching in awake headfixed mice. Current clamp recording from a layer-4 cortical neuron in barrel cortex of an awake headfixed mouse showing persistent depolarization of membrane potential during active whisking (periods of whisker movements indicated by black bar). Access resistance 37 MΩ; input resistance, 88 MΩ; depth of cell 468 μm below surface of the brain. **(g–h)** Simultaneous whole cell recording and optogenetic stimulation *in vivo*. **(g)** Jaws-expressing neuron in cortex showing hyperpolarization at onset of red light delivery. Adapted from ref [26]. **(h)** Channelrhodopsin-2 expressing cortical neuron in a Thy1-ChR2 mouse, showing evoked spiking in response to 20ms blue light pulses. All animal use complied with institutional and federal regulations. (g) adapted from Chuong et al Nat Neuroscience 2014[26].

Table 1

Troubleshooting

Step	Problem	Reason and solution
Step 30: Monitor currents and de-noise the autopatcher	Baseline current is unstable and drifts >100pA/min are observed.	1. Bad ground electrode: Ensure the ground wire has proper connectivity, and Ag-AgCl pellet is soldered properly to the ground wire. Older pellets also benefit from re-chloriding to refresh their active surfaces. 2. Inadequate internal solution in the pipette: Ensure the pipette has been filled with enough internal solution to submerge a portion of the Ag-AgCl wire. 3. Inadequate ACSF bath: ensure both the ground electrode's Ag-AgCl pellet and the pipette tip are submerged in the ACSF bath. 4. Poor conductivity of the silver wire inside the pipette holder: Make sure that the silver wire in the pipette holder is properly chlorided. Soaking the wire in bleach for 3–5 minutes, followed by thorough cleaning in distilled water, is sufficient to correct this problem. 5. Broken silver wire inside the pipette holder: Check the electrical continuity between the gold coated pin on the pipette holder and the silver wire using a multimeter.
	Peak-to-peak noise level is greater than 40pA	1. 50 or 60 Hz electrical noise sources inside the Faraday cage: ensure all sources of 50 or 60 Hz noise have been turned off or removed from the Faraday cage and all ground loops are identified and eliminated. Add grounded shielding as necessary.
	Current trace is modulated at low frequencies (0.25–6 Hz)	1. Improper ground wire placement: ensure the ground wire has proper connectivity and that the Ag-AgCl pellet is soldered properly to the ground wire, checking using a multimeter. Ensure the Ag-AgCl pellet is on the skull, surrounded by conductive saline. 2. Mechanical disturbance caused by improper air table flotation, or equipment that is not rigidly attached to the table: Ensure the vibration isolation air table is floating on pressurized air and all components of the autopatcher have been fastened rigidly to the air table. 3. Movement of skull due to improper headplate fixation: Ensure the headplate is rigidly attached to the skull and there is no relative motion between them when the mouse is headfixed in the custom holder. Using a pair of tweezers, lightly touch the skull while looking through the stereomicroscope to observe any relative motion between the skull and the dental acrylic. Autopatching should not be attempted if the dental acrylic has detached from the skull or the headfixation is inadequate.
Step 32 and BOX 2, Autopatching Step 1: Checking pipette outside the brain	The pipette resistance is not within the optimal range for autopatching (3–9 MΩ):	1. Sub-optimal pipette pulling program settings: Program the pipette puller to pull pipettes with resistances in the range of 3–9 MΩ In our laboratory we have obtained best results with pipettes with resistances in the range of 5–7 MΩ. Also, see Figure 3 for examples of pipette tips.
	The variation in pipette resistance is greater than 50 KΩ:	1. Particulates in the pipette: Always ensure the pipette internal solution is filtered with a 0.2 μm filter before backfilling the pipette. Use a new filter and a new syringe for every experiment. 2. Particulates introduced during backfilling of pipettes: During an experiment, keep the Microfil away from dust or lint, by storing the Microfil and syringe in an enclosed container. Store the Microfil in filtered 70% ethanol solution when not in use during an experiment. Leaving the Microfil outside overnight may result in the accumulation of particulates at the tip of the Microfil that may end up clogging the pipettes internally, affecting impedance measurements during autopatching. Clean the Microfil using deionized water, ethanol, and lens paper. 3. Particulates introduced from electrode holder: Remove the electrode holder from the headstage and clean it by washing it in 0.2 μm filtered 70% ethanol followed by a wash in filtered de-ionized water. 4. AgCl debris inside the pipette: When installing the pipette into the holder, the AgCl on the electrode wire might get dislodged and clog the pipette tip. Clean the electrode wire using lens paper soaked in 70% ethanol. Make sure that the wire is fully dry before replacing it.
Step 33 and BOX 2, Autopatching Step 2:	High fraction (>20%) of pipettes gets blocked/ clogged during regional pipette localization:	1. Age of the mice: Best results are obtained with mice between 8–12 weeks old. Older mice may result in higher rate of clogging during the descent to depth, affecting the yield. 2. Condition of the craniotomy: Ensure the craniotomy is clean and moist at all times and there are no debris or blood on the brain surface. 3. Insufficient high positive pressure: Increase the high positive pressure setting on the autopatcher control box to 1000 mBar if blocking/clogging persists. Such higher pressures can also be used to keep the pipette tip clean if targeting deeper brain structures below the cortex. 4. Check whether the dura has been removed at the point of entry of the pipettes. If not, carefully repeat **Step 19** at the desired entry point.
	A significant fraction of pipettes (>5%) get broken during the descent to depth.	1. Improper positioning of pipette tip at the start of autopatching: Ensure that the pipette tip is positioned at the center of the craniotomy and that it is not touching the skull at the edges of the craniotomy. For proper visualization, you could drain the ACSF temporarily during this step as refraction can make it difficult to visualize the pipette tip and the brain using the stereomicroscope. Once positioned, add ACSF as soon as possible to prevent tissue drying.

Step	Problem	Reason and solution
		2. Bone fragments, debris in the craniotomy: Periodically check the craniotomy for any debris or bone fragments that might have been introduced at the brain surface. Wash with ACSF to clean.
BOX 2, **Autopatching Step 3: neuron hunting**	Resistance traces are not flat-lined and exhibit variance greater than 100 KΩ.	1. Movement of skull due to improper headplate fixation: See TROUBLESHOOTING **Step 30**. 2. Excess movement of the brain relative to the skull: if there is visible motion of the brain tissue through the stereomicroscope due to heartbeat or breathing, the tissue is unsuitable for autopatching. This can be caused by damage to the brain tissue while performing the craniotomy in **Step 18**. Ensure the brain surface is not damaged in any way while performing the craniotomy or while installing the pipettes in the autopatcher during autopatching. Also ensure the animal is maintained at proper anesthetic plane throughout the experiment and its body temperature is properly regulated. Labored breathing, from too much anesthetic, is not good for the animal, and causes motion as well. The breathing rate should be faster than ~0.5 Hz. Labored breathing could also be caused by improper posture of the animal. If the head is too low relative to the body or the animal is resting its weight on the chest area, it can increase labored breathing. For 8 week old C57BL/6 mice, the top of the skull should be about 25 mm from the heating pad beneath the mouse and the heating pad should allow for lung expansion without causing excessive motion of the spine. 3. Internal clogging of pipette: See TROUBLESHOOTING **Step 30**.
Step 34 and 35; and BOX 2, **Autopatching Step 4 and 5: Gigasealing**	Significant fraction of neuron hunting (>60%) attempts result in false positives or in seals less than 100 MΩ	1. Movement of skull due to improper headplate fixation: See TROUBLESHOOTING **Step 30**. 2. Excessive movement of the brain relative to the skull: See TROUBLESHOOTING BOX 2, **Autopatching Step 3: neuron hunting**. 3. Default **'Neuron detection threshold (M-Ohms)'** of 0.25 MΩ is insufficient to eliminate false positives: The neuron detection threshold was found in our original study to be optimal at 0.25 MΩ. However, this might be insufficient to eliminate false positives arising due to high variance in pipette resistance (as described in TROUBLESHOOTING for **Step 32**). Increase the **'Neuron detection threshold (M-Ohms)'** in the autopatcher software GUI to a value between 0.3–0.75 MΩ to mitigate this.
	Low percentage (<30%) of successful gigaseals	1. Movement of skull due to improper headplate fixation: See TROUBLESHOOTING **Step 30**. 2. Excessive movement of the brain relative to the skull: See BOX 2, **Autopatching Step 3: neuron hunting**. 3. Sub-optimal condition of the craniotomy: Ensure that the brain surface is kept moist with application of ACSF at all times during the experiment so as to keep the tissue healthy. Ensure that the brain surface is not accidentally damaged while performing the craniotomy in **Step 18**, or when pipettes are inserted during autopatching. 4. Sub-optimal pipette tip geometry: If a significant fraction of trials result in resistance increasing to 40–100 MΩ, without forming a gigaseal, it may be indicative of a too-large pipette tip diameter. Refer to the pipette puller user manual to make changes to the program to get pipettes with smaller tips (with corresponding increase in resistance of 0.5–1 MΩ). For instance, in the Sutter P97 puller, this can sometimes be achieved by increasing the velocity setting in the pulling program by 1–2 points.
Step 36	Significant fraction (>20%) of gigasealed cells is lost during breaking in process.	1. Break-in process is too harsh on the cell: If the cell is lost when attempting to break in, the break-in vacuum pressure might be too high. Use a smaller value of high negative pressure (−150 to −200 mBar) during break-in. Alternatively, the **'zap'** function in the Multiclamp Commander software can be used to send a sharp voltage pulse to electroporate the membrane to break in. Start by using short zap pulses (25 μs) and increase the zap durations until break-in is achieved.
Step 37–39	Significant fraction (>10%) of whole cell patched cells are lost/become too leaky with 5 minutes of autopatching.	1. Movement of skull due to improper headplate fixation: See TROUBLESHOOTING **Step 30**. 2. Excessive movement of the brain relative to the skull: See TROUBLESHOOTING BOX 2, **Autopatching Step 3: neuron hunting**. 3. Sub-optimal condition of the craniotomy: Ensure that the brain surface is kept moist with application of ACSF at all times during the experiment so as to keep the tissue healthy. Ensure that the brain surface is not accidentally damaged while performing the craniotomy in Step 6, or when pipettes are inserted during autopatching and that excessive bleeding is not observed during the autopatching experiment. 4. The pipette solution is prepared improperly: Ensure the osmolarity of the pipette solution is as close to 290 mOsm as possible. Maintain the solution on ice throughout the experiment to preserve the ATP and GTP. This will increase the effective duration of the recordings.